Bi-Annual Report
Final Results
Geochemical Analysis of Coso Geothermal System
China Lake, California
FY 2012

Contract N68936-07-C-0073
Kelly Blake, Kelly.blake@navy.mil phone: 760-939-4056
Department of the Navy, China Lake Naval Air War Center Weapons Division,
429 E. Bowen Rd. BLDG 982, Mail Stop 4011
China Lake, CA 93555-6108
F.O.B. Destination: Geothermal Program Office,
429 East Bowen Road, China Lake, CA 93555-6108

January 25, 2013

by GEOLOGICA Inc.
DUNS Number: 830053760
CAGE Code: 3HNZ4
Active CCR Registration
Active ORCA Registration
TIN: 94-332629

Executive summary

This report presents the geochemical data collected from production and injection wells of the Coso Geothermal System during the calendar year 2011. The data were collected by the Coso Operating Company (COC), and provided to GEOLOGICA by the Navy. GEOLOGICA has evaluated the geochemical monitoring data and assessed variations in geochemical parameters over space and time. This report focuses on using the geochemical data to better understand reservoir conditions such as injection response, temperature distribution, and boiling in the reservoir.

During the last year, COC continued injection of significant amounts of groundwater from Hay Ranch in Rose Valley into the Coso geothermal reservoir for purposes of reducing the negative net withdrawal of geothermal fluids from the reservoir and related pressure decline thereby mitigating the decline in steam production. The chemical, temperature, and pressure response of the field in response to this new groundwater injection program was monitored by COC and the data were transmitted to GEOLOGICA.

In addition to conducting field-wide geochemical analysis, geochemical data from East Flank and West Field injection and production wells were assessed in an effort to better understand the reservoir and feedzone of those production areas. This work is expected to continue through the next fiscal year, broadening in focus to other areas of the production field. Ongoing objectives include using geochemical data to (1) help track the long term reservoir trends in temperature, liquid saturation, area separation and mixing, (2) assess the effect of injection on the reservoir conditions, and (3) evaluate the distribution, breakthrough, and returns of the injectate.

This evaluation provided the following conclusions:

- Cl has remained consistent in reservoir fluid from 2010 to 2011. Some small increases and decreases have occurred that can be attributed to local injectate source and volume. No substantial changes have been observed in BLME, BLMW, East Flank, or Navy I. Cl has slightly decreased over time in Navy II since 2010. Since production began, Cl concentrations have been relatively constant in various areas of the reservoir.
- With the exception of extreme spikes related to wells drying out, shifts in Cl concentration trends in production fluid appear to correlate with changes in average Cl concentration levels in injection fluid in the power plant areas.
- Currently, Cl concentrations in the Coso reservoir liquid are ≥ Cl concentrations in injection fluids suggesting that while long term injection recharge produces Cl increases, Cl increases alone can't be attributed to injection breakthrough. These increases could be related to concentration by boiling.
- Historically, the Cl/B ratio has been higher in the southern part of the Coso reservoir relative to the central and eastern parts. The Cl/B in the injectate followed the same pattern with the highest Cl/B fluids (waste brine) injected in the south and the highest Cl/B in produced fluids near the injection wells with high brine injection volumes, suggesting that Cl/B reflects injection. In 2011, this

pattern changed for injectate but not produced brine; injectate with the highest Cl/B ratios (Hay Ranch water) was injected into the center of the Navy I area and in the East Flank, but the pattern of Cl/B in produced fluids remained unchanged. However, this chemical pattern may provide a tracer of injectate in produced brine.

- The gas/steam (G/S) ratio in produced steam has changed little since 2010. The most significant G/S increases occurred in Navy II. In Navy I, BLME, and BLMW, G/S has remained stable with a small number of wells increasing and a small number decreasing. Decreases may be related to injection-derived steam. Across the field, G/S generally continued to increase in the center of the field and decrease on the edges. Noncondensible gases (NCG) in reservoir fluid followed a similar pattern.
- H_2S/CO_2 ratios vary significantly across the field, but have not varied over time in individual wells despite changes in boiling and enthalpy. Higher relative concentrations of trace gases on the edges of the field may reflect vapor recharge.
- Ratios of H_2S/CO_2, H_2/CO_2, and CH_4/CO_2 remained high on the outside of the field and low in the center, but showed different patterns. While H_2/CO_2 was highest in the east-north, CH_4/CO_2 was highest in the west and south and H_2S/CO_2 follows enthalpy being higher where wells still produce brine.
- Available isotope data, such as Oxygen-18 ($\delta^{18}O$) and Deuterium (δD) data indicate that using isotopes as injection tracers may require understanding the temperature of boiling and will probably require additional data. Data from 2011 suggest that reservoir fluids boil at approximately 190-200°C (374-392°F).
- Cation (NaKCa) and quartz brine geothermometers remained relatively stable. In the past both geothermometers showed similar spatial patterns, but NaKCa was consistently higher than quartz, suggesting that differences between deep temperatures (NaKCa) and near-wellbore temperatures (quartz) may be narrowing.
- Gas geothermometers remained consistent, maintaining the correlation with measured enthalpy. Enthalpy and the number of steam wells were approximately constant: a small number of wells shifted to steam wells while a small number of steam wells shifted to two phase, resulting in no large net change across the field.
- Evaluation of measured static and dynamic temperatures, brine and gas geothermometers, and measured enthalpy indicate that enthalpy and gas geothermometers appear to reflect the rock temperatures whereas dynamic surveys and brine geothermometers reflect near well reservoir liquid temperatures. It appears that rock temperatures remain high enough to boil reservoir liquid and add excess steam to total fluid discharge.
- Vapor saturation in the reservoir is indicated by (1) "y", calculated using noncondensible gas chemistry (GRID method), (2) differences between dynamic and static feed zone temperatures, and (3) simple mixing to produce observed G/S in the Navy I steam zone, indicate that there is approximately an average 25% by weight vapor saturation in the reservoir.
- Vapor saturation based on WATCH geochemical modeling program indicates that vapor saturation in the reservoir is slightly higher at an average of 30% across

wells that possessed enough sampling data to run the program (19 wells across all areas of the field with an emphasis on the East Flank).

- In most of the field, comparison of Cl, G/S and enthalpy suggests excess steam is produced by adding reservoir vapor that is in equilibrium with reservoir brine to fluid flowing to the wells (as excess steam (enthalpy) increases, chloride and G/S do not). In the East Flank and BLM East, the source of excess steam appears to be additional boiling of fluid as it flows through hot rock (as excess steam (enthalpy) increases, chloride increases, and G/S goes either way). These areas may be more conducive to generating injection-derived steam.

Table of contents

Executive summary iii
1. Introduction 1
1.1. Summary of data received 1
1.2. Database and GIS 2
1.3. Data QA/QC 4
2. Methodology and analysis 5
2.1. Brine-liquid data – Temporal and spatial analysis 5
2.2. Steam NCG data – Temporal and spatial analysis 5
2.3. Additional data evaluation 6
2.3.1. Injection response 6
2.3.2. Reservoir temperatures 7
2.3.3. Boiling, phase segregation, and reservoir liquid saturation 7
2.3.4. Isotopes 8
3. Observations, evaluation and discussion 9
3.1. Temporal and spatial trends 9
3.2. Chemical indications of injection response 9
3.2.1. Chloride 10
3.2.2. Chloride / Boron 12
3.2.3. Gas/Steam and gas composition 14
3.2.4. Isotopes 16
3.3. Temperature 19
3.3.1. NaKCa geothermometers 19
3.3.2. Quartz geothermometers 19
3.3.3. Gas geothermometers 20
3.3.4. Gas vs. Cation geothermometers 20
3.3.5. Temperature summary 21
3.3.6. Measured temperatures 21
3.4. Steam wells and boiling 23
3.4.1. Steam wells 23
3.4.2. Measured enthalpy 23
4. Boiling, phase segregation, and liquid saturation 24
4.1. Boiling model 24
4.2. Dynamic versus static temperatures 26
4.3. Y-values 26
4.4. Mechanism of excess steam 29
4.5. Reservoir vapor saturation in the reservoir from geochemical modeling 33
5. Conclusions and next steps 35
6. References 38
Figure Attachments 1

Appendix 1. Coso Geothermal System 2011 Raw Data

List of Tables

Table 2-1. Average Chemical Composition of Injection Fluid Types at Coso 6
Table 3-1. Average Cl/B Ratio of Injection Fluids at Coso 13
Table 4-1. WATCH calculated reservoir steam saturation 2010-2011 34

List of Figures

Figure 3-1. Comparison of chloride in injectate and reservoir brine in BLME. Historical injection data is before the Hay Ranch injection project. 11
Figure 3-2. Cl/B in 2011-produced reservoir fluids and injection (all injection fluids) .. 14
Figure 3-3. Stable isotope data of the Coso Geothermal System in 2011 17
Figure 3-4. 38C-9 Trends in Oxygen-18 and Deuterium with injection over time 18
Figure 3-5. Downhole static reservoir temperature (°C) versus measured enthalpy (kJ/kg) (left Y-axis) and downhole dynamic temperatures (°C) (right Y-axis) 22
Figure 4-1. Changes in G/S derived from variable fraction of single-stage boiling of reservoir liquid equivalent to brine wells 25
Figure 4-2. Grid Y-values for 2011 based on gas equilibrium FT (CH_4 breakdown to CO_2 and H_2) and HSH (H_2-H_2S reaction) 27
Figure 4-3. Y-grid for 2011 Production Wells (after Truesdell & D'Amore, 1985) 28
Figure 4-4. Well 37-17 measured enthalpy (kJ/kg) vs Cl in mg/kg in brine and corrected to total flow, and gas/steam (G/S in ppm) in steam 31
Figure 4-5. Well 16B-20 measured enthalpy (kJ/kg) vs Cl in mg/kg in brine and corrected to total flow, and gas/steam (G/S in ppm) in steam 32

List of Figure Attachments

Figure A 1. Steam wells in 2011 2
Figure A 2. NaKCa Geothermometer Temperatures vs. Injection in 2011 3
Figure A 3. Changes in NaKCa geothermometer temperatures from 2010 to 2011 4
Figure A 4. NaKCa geothermometer temperature contours in 2011 5
Figure A 5. 2011 Quartz geothermometer temperatures vs. injection 6
Figure A 6. Changes in quartz geothermometer temperatures 2010 to 2011 vs. injection total volume, 2011 7
Figure A 7. Quartz geothermometer temperatures, 2011 8
Figure A 8. Methane geothermometer temperature contours, 2011 9
Figure A 9. Ammonia geothermometer temperature contours, 2011 10
Figure A 10. Geothermometers and measured enthalpy in wells with less than 10% excess steam 11
Figure A 11. Geothermometers and measured enthalpy in wells with 20-80% excess steam 12
Figure A 12. Geothermometers and measured enthalpy in wells with 80-100% excess steam 13
Figure A 13. 10-year change in measured Noncondensible Gas, 2001-2011 14
Figure A 14. 10-year change in measured Enthalpy, 2001-2011 15
Figure A 15. 10-year change in Reservoir Chloride concentration, 2001-2011 16

Figure A 16. 10-year change in NaKCa Geothermometer Temperatures, 2001-2011 17
Figure A 17. 10-year change in Quartz Adiabatic Geothermometer Temperatures, 2001-2011 18
Figure A 18. Changes in injection from 2010 to 2011 19
Figure A 19. Reservoir chloride concentration in BLM East Wells since 1987..... 20
Figure A 20. Reservoir chloride concentration in BLM West Wells since 1987 21
Figure A 21. Reservoir chloride concentration in East Flank Wells since 1987 22
Figure A 22. Reservoir chloride concentration in Navy I Wells since 1987 23
Figure A 23. Reservoir chloride concentration in Navy II Wells since 1987..... 24
Figure A 24. Chloride/Injection Map 2011..... 25
Figure A 25. Changes in Chloride vs. Injection 2011..... 26
Figure A 26. Chloride concentrations in injection fluids, 2011..... 27
Figure A 27. 2011 Coso Injection and Production Wells, including wells injected with Hay Ranch Water..... 28
Figure A 28. Corrected chloride concentrations in production wells, 2011 29
Figure A 29. Calculated (via WATCH) aquifer chloride concentrations 2011 30
Figure A 30. Calculated aquifer chloride concentrations overlain by injection fluid chloride concentrations, 2011 31
Figure A 31. Aquifer chloride concentrations overlain by measured enthalpy, 2011 32
Figure A 32. Chloride/Boron ratios in 2011 compared to injection 33
Figure A 33. Chloride/Boron ratios in injection fluid, 2011..... 34
Figure A 34. Chloride/Boron production contour map for 2011 35
Figure A 35. Calculated (via WATCH) chloride/boron ratios in aquifer fluid, 2011 36
Figure A 36. Calculated aquifer chloride/boron ratios overlain by injection fluid chloride/boron ratios, 2011 37
Figure A 37. Calculated aquifer chloride/boron ratios overlain by injection fluid chloride/boron ratios, 2010 38
Figure A 38. Measured chloride/boron ratios over time with average injection fluid chloride/boron ratios, BLME 39
Figure A 39. Measured chloride/boron ratios over time with average injection fluid chloride/boron ratios, BLMW..... 40
Figure A 40. Measured chloride/boron ratios over time with average injection fluid chloride/boron ratios, Navy I 41
Figure A 41. Measured chloride/boron ratios over time with average injection fluid chloride/boron ratios, Navy II..... 42
Figure A 42. Measured chloride/boron ratios over time with average injection fluid chloride/boron ratios, East Flank 43
Figure A 43. Measured noncondensible gas (NCG) contours in 2011 based on all wells measured 44
Figure A 44. Change in Noncondensible Gas, 2011..... 45
Figure A 45. 26-9 Geochemical Constituents vs Time with Injection 46
Figure A 46. 26A-9 Geochemical Constituents vs Time with Injection..... 46
Figure A 47. 38-9 Geochemical Constituents vs Time with Injection 47
Figure A 48. 38B-9 Geochemical Constituents vs Time with Injection..... 47
Figure A 49. 38C-9 Geochemical Constituents vs Time with Injection..... 48
Figure A 50. 38D-9 Geochemical Constituents vs Time with Injection..... 48

Figure A 51. 42A-16 Geochemical Constituents vs Time with Injection..... 49
Figure A 52. 42B-16 Geochemical Constituents vs Time with Injection..... 49
Figure A 53. 83A-16 Geochemical Constituents vs Time with Injection..... 50
Figure A 54. 83B-16 Geochemical Constituents vs Time with Injection..... 50
Figure A 55. 16-20 Geochemical Constituents vs Time with Injection 51
Figure A 56. 33-19 Geochemical Constituents vs Time with Injection 51
Figure A 57. 37B-17 Geochemical Constituents vs Time with Injection..... 52
Figure A 58. 58B-18 Geochemical Constituents vs Time with Injection..... 52
Figure A 59. 63B-7 Geochemical Constituents vs Time with Injection..... 53
Figure A 60. 65A-18 Geochemical Constituents vs Time with Injection..... 53
Figure A 61. 68-6 Geochemical Constituents vs Time with Injection 54
Figure A 62. 78-7 Geochemical Constituents vs Time with Injection 54
Figure A 63. 81-18 Geochemical Constituents vs Time with Injection 55
Figure A 64. 87A-7 Geochemical Constituents vs Time with Injection..... 55
Figure A 65. Ratio of hydrogen sulfide to carbon dioxide in 2011 56
Figure A 66. Ratio of hydrogen gas to carbon dioxide in 2011..... 57
Figure A 67. Ratio of methane to carbon dioxide in 2011 gas data..... 58
Figure A 68. Gas/Steam Ratio in BLME since 1987..... 59
Figure A 69. Gas/Steam Ratio in BLMW since 1987 59
Figure A 70. Gas/Steam Ratio in East Flank since 1999..... 60
Figure A 71. Gas/Steam Ratio in Navy I since 1999..... 60
Figure A 72. Gas/Steam Ratio in Navy II since 1999..... 61
Figure A 73. Reservoir NCG in BLME since 1999..... 61
Figure A 74. Reservoir NCG in BLMW since 1999 62
Figure A 75. Reservoir NCG in East Flank since 1999..... 62
Figure A 76. Reservoir NCG in Navy I since 1999..... 63
Figure A 77. Reservoir NCG in Navy II since 1999..... 63
Figure A 78. CO_2 compared to H_2S, NH_3, H_2 and CH_4 for all wells since 1999..... 64
Figure A 79. CO_2 vs. NH_3 for all wells since 1999 64
Figure A 80. CO_2 vs. CH_4 for all wells since 1999..... 65
Figure A 81. CO_2 vs. H_2 for all wells since 1999 65
Figure A 82. CO_2 vs. H_2S for all wells since 1999 66
Figure A 83. Ratio of H_2S/CO_2 over time..... 66
Figure A 84. 26-9 Stable Isotopes..... 67
Figure A 85. 38C-9 Stable isotopes 67
Figure A 86. 42A-16 Stable isotopes..... 68
Figure A 87. 83B-16 Stable isotopes 68
Figure A 88. 26-9 Stable Isotopes vs Time with Injection 69
Figure A 89. 26A-9 Stable Isotopes vs Time with Injection 69
Figure A 90. 38-9 Stable Isotopes vs Time with Injection 70
Figure A 91. 38B-9 Stable Isotopes vs Time with Injection..... 70
Figure A 92. 38C-9 Stable Isotopes vs Time with Injection..... 71
Figure A 93. 38D-9 Stable Isotopes vs Time with Injection 71
Figure A 94. 42A-16 Stable Isotopes vs Time with Injection 72
Figure A 95. 42B-16 Stable Isotopes vs Time with Injection..... 72
Figure A 96. 83A-16 Stable Isotopes vs Time with Injection 73

Figure A 97. 83B-16 Stable Isotopes vs Time with Injection..... 73
Figure A 98. 63B-7 Stable Isotopes vs Time with Injection..... 74
Figure A 99. 78-7 Stable Isotopes vs Time with Injection 74
Figure A 100. 81-18 Stable Isotopes vs Time with Injection 75
Figure A 101. 87A-7 Stable Isotopes vs Time with Injection 75
Figure A 102. Measured enthalpy contours in 2011..... 76
Figure A 103. Measured enthalpy in BLME since 1987 77
Figure A 104. Measured enthalpy in BLMW since 1987..... 77
Figure A 105. Measured enthalpy in East Flank since 1987 78
Figure A 106. Measured enthalpy in Navy I since 1987 78
Figure A 107. Measured enthalpy in Navy II since 1987..... 79
Figure A 108. Grid calculated Y contours in 2011..... 80
Figure A 109. Chloride-enthalpy-gas/steam trends in well 16A-20, in BLM East 81
Figure A 110. Chloride-enthalpy-gas/steam trends in well 16B-20, in BLM East..... 81
Figure A 111. Chloride-enthalpy-gas/steam trends in well 32-20, in BLM East 82
Figure A 112. Chloride-enthalpy-gas/steam trends in well 34-20, in BLM East 82
Figure A 113. Chloride-enthalpy-gas/steam trends in well 34A-20, in BLM East 83
Figure A 114. Chloride-enthalpy-gas/steam trends in well 23-19RD, in BLM West 83
Figure A 115. Chloride-enthalpy-gas/steam trends in well 33-19, in BLM West..... 84
Figure A 116. Chloride-enthalpy-gas/steam trends in well 33B-19, in BLM West 84
Figure A 117. Chloride-enthalpy-gas/steam trends in well 58B-18, in BLM West 85
Figure A 118. Chloride-enthalpy-gas/steam trends in well 74A-19, in BLM West..... 85
Figure A 119. Chloride-enthalpy-gas/steam trends in well 74B19RD, in BLM West..... 86
Figure A 120. Chloride-enthalpy-gas/steam trends in well 81B-19, in BLM West 86
Figure A 121. Chloride-enthalpy-gas/steam trends in well 43-7, in Navy I..... 87
Figure A 122. Chloride-enthalpy-gas/steam trends in well 43A-7, in Navy I..... 87
Figure A 123. Chloride-enthalpy-gas/steam trends in well 52B-7, in Navy I..... 88
Figure A 124. Chloride-enthalpy-gas/steam trends in well 68-6, in Navy I..... 88
Figure A 125. Chloride-enthalpy-gas/steam trends in well 15-17RD, in Navy II..... 89
Figure A 126. Chloride-enthalpy-gas/steam trends in well 37-17, in Navy II 89
Figure A 127. Chloride-enthalpy-gas/steam trends in well 37A-17, in Navy II..... 90
Figure A 128. Chloride-enthalpy-gas/steam trends in well 63A-18, in Navy II..... 90
Figure A 129. Chloride-enthalpy-gas/steam trends in well 64A-18, in Navy II..... 91
Figure A 130. Chloride-enthalpy-gas/steam trends in well 76A-18, in Navy II..... 91
Figure A 131. Chloride-enthalpy-gas/steam trends in well 38-9, in East Flank..... 92
Figure A 132. Chloride-enthalpy-gas/steam trends in well 38B-9, in East Flank 92
Figure A 133. Chloride-enthalpy-gas/steam trends in well 38C-9, in East Flank 93
Figure A 134. Chloride-enthalpy-gas/steam trends in well 83B-16, in East Flank 93

1. Introduction

This report presents work completed under GEOLOGICA's contract with the Navy (Contract No. N68936-07-C-0073) to provide geochemical evaluation of the geothermal fluid chemistry of the Coso Geothermal System at China Lake. This report is the second installment of 2012, under Contract Item 0005AB and is a presentation of findings, data, and observations. This report includes figures and observations of geochemical and related physical data from Coso injection and production fluids provided by Coso Operating Company (COC) collected during the 2011 calendar year.

The evaluation of geochemical monitoring data from Coso under Navy contract has occurred for more than 10 years, initially by the Energy and Geoscience Institute (EGI) and subsequently by GEOLOGICA. During this period an extensive database has been established, including a Geographic Information System (GIS) database. This work was initially focused on brine chemistry and many of the analytical and graphical methods were based on brine analysis. Examination of steam chemistry, especially gas analysis, began with 2006 calendar year data. The objectives of the work are two-fold: (1) monitor trends in reservoir conditions indicated by geochemistry, and (2) develop new and/or improved methods for evaluating geochemical monitoring data.

This report is intended to provide a summary of the current status of the geochemical conditions in the Coso Geothermal System. This report focuses on temporal and spatial trends in geochemical parameters. Since part of the scope of work includes improving or developing new methods of evaluating reservoir processes using fluid chemistry, this report also presents a few methods for interpreting reservoir processes or conditions from geochemical data, and our initial attempts to apply them at Coso. These interpretations are focused on understanding the geochemical changes related to changes in reservoir conditions and on developing methods to use observed geochemical changes to help monitor and manage changes related to reservoir conditions such as vaporization, drying, and injection response.

This report includes: the formal geochemical data QA/QC; a description of the process and methodology of this evaluation; observations and analysis of the data; conclusions and recommendations; and the database in electronic format. Some of the preliminary geochemical evaluation methods discussed herein are still evolving: recommendations for further development are included.

1.1. Summary of data received

Chemical analyses of the steam and liquid phases (if liquid is produced) from each Coso production well were provided for the 2011 calendar year (Appendix 1). GEOLOGICA received the 2011 geochemical data from Coso in late spring 2012. These data include brine and steam analyses with sampling conditions and measured total wellhead enthalpy from most of the 72 Coso production wells. In addition, injection chemistry from

quarterly samples collected from 28 injection wells was provided. Sampling conditions and measured enthalpy are required for the interpretation of the geochemical results. Due to scheduling conflicts and the ability to alternatively calculate enthalpy, enthalpy was not measured in any 100% steam wells in 2011; instead, enthalpy was calculated in 47 steam wells based on wellhead pressure and temperature using steam tables.

Brine analyses include sodium (Na), potassium (K), calcium (Ca), lithium (Li), arsenic (As), boron (B), silica (SiO_2), bicarbonate (HCO_3), chloride (Cl), fluoride (F), sulfate (SO_4), total dissolved solids (TDS) and pH. Steam analyses include total gas/steam (G/S), carbon dioxide (CO_2), hydrogen sulfide (H_2S), ammonia (NH_3), argon (Ar), methane (CH_4), and hydrogen (H_2). All analyses of production brine and steam are in ppmw (parts per million by weight) with the exception of stable isotopes, which are in $^0/_{00}$. Injection fluid is analyzed in milligrams per kilogram (mg/kg). Sampling conditions include the date, total enthalpy of the well discharge, and steam and brine separation and collection temperatures.

The 2011 data set includes 155 gas samples from 69 operating production wells and 75 brine samples from 22 of those wells that are producing brine (including a number of duplicates). Enthalpy data for 2011 were provided for 27 two-phase wells, plus the calculated enthalpies from the 47 additional 100% steam wells. In addition, daily injection volumes and quarterly geochemical samples were collected from 28 injection wells.

1.2. Database and GIS

The Navy Geothermal Program Office (GPO) Coso originally established a geothermal geochemistry database (MS ACCESS-based), which transferred geochemical data to a database linked to a Geographic Information System (GIS) of the Coso geothermal well field. The GIS and databases were established in the previous contract for this work. However, because of evolving technology, increasing functionality, and efficient user interface of Microsoft Excel, all current and historical data was transferred to and processed with a Microsoft Excel database starting with data year 2010.

The geochemical database includes analytical results from steam and brine production well samples as well as analyses of liquid samples of injection fluid. Analytical data in the database is typical of basic geothermal analysis and can include:

- Brine: Sampling conditions (sampling pressure, temperature and enthalpy), date, TDS, Na, K, Ca, SiO_2, B, Li, As, HCO_3, Cl, SO_4, and F
- Steam: Sampling conditions (sampling pressure, temperature and enthalpy), date, Gas/steam (G/S) ratio, CO_2, H_2S, NH_3, Ar, N_2, CH_4, and H_2
- Injection fluid (Sampled quarterly): Date, Na, K, Ca, Li, Mg, Sr, B, SiO_2, As, Cl, F, SO_4, HCO_3, pH, and TDS

This database is capable of adding parameters for various well sampling locations should additional data become available. The database system processes the data and is capable of performing the following functions:

1) Culls the raw data for bad charge balances and air contamination
2) Calculates geothermometer temperatures
3) Correlates water and gas analyses
4) Corrects raw steam and brine data to reservoir conditions based on steam fraction
5) Uses the geothermometer temperatures and measured enthalpy to compensate for concentration changes due to boiling and excess steam
6) Calculates parameters such as the excess steam fraction and the geothermometer enthalpies

The database is used to create thematic maps of parameters such as changes in chloride concentrations, geothermometer temperatures, and reservoir boiling. The purpose of the thematic maps is to monitor and document any changes in the reservoir chemistry resulting from exploitation with respect to surface location within the reservoir. Reservoir chemistry changes can indicate the incursion of cooler waters (Ellis and Mahon, 1977), the flow of injected water (which is required for pressure maintenance (Stefansson, 1997)), and the excessive flow of injection water (which would cool parts of the reservoir too quickly). The choice of the parameters was derived from several discussions in the literature of observed and theoretical chemical changes in exploited geothermal reservoirs (Abrigo et al., 2002; Ellis and Mahon, 1977; Harper and Jordan, 1985; Henley, 1984a; Henley, 1984b).

The functionality of the monitoring database was greatly increased by joining it to a GIS database of the Coso geothermal field during the fourth year of the first contract and conversely the geochemical database to Excel in 2010. A map of the field was digitized using the computer program ARC/INFO. Seven coverages were created: 1) well courses, 2) well heads, 3) production intervals, 4) well pads, 5) roads, 6) unit boundaries, and 7) section lines. The depths of the production intervals were chosen by picking the highest density of lost circulation zones along the well course. If the density distribution was uniform, the midpoint of the well course was chosen. Well courses and midpoints were updated this year to include recently drilled and active wells.

Beginning in 2008, the GIS database was used to spatially contour field-wide concentrations, temperatures, ratios, and changes over time. The application of this process has continued to increase annually as the monitoring data analysis has evolved. Beginning in 2010, this process was used to more specifically evaluate the influence of the Hay Ranch groundwater being injected into areas of the field.

This year the GEOLOGICA Team updated the database to include the 2011 geochemical data. The 2011 data were processed using updated formulas first incorporated in the FY2010 Geochemical Monitoring Report. Analysis in that report discovered flaws in

previous algorithms causing calculation issues in data, particularly when correcting data back to reservoir conditions. All available past and present raw data were transferred to the "Coso Geochemistry Database.xls" database using Microsoft Excel, where they were processed including two-phase wells and those wells that produce 100% steam. The data for 100% steam wells were not included in the database until FY2008, because the conditions under which the steam was produced were unknown, and thus the reservoir composition could not be calculated. The new database includes the data in the concentration units required for calculation of the gas geothermometers as well as the results of the calculations.

Data were contoured in ArcView GIS using the natural neighbor interpolation algorithm (ESRI, 2008). The method is a local interpolator; interpolated heights are within the range of the samples used. Interpolation values are determined by weights based on proportionate areas defined by Voronoi polygons derived from the distribution of sample points (ESRI, 2008). Values at surveyed locations are retained and a smooth surface is generated between sample points. The resulting interpolated surface does not extend beyond the sample point locations. The GIS database will be provided on CD with the final report.

1.3. Data QA/QC

A QA/QC review of the 2011 geochemical monitoring data provided by the Navy GPO was performed as the data were entered into the database. All brine analyses showed a charge balance of zero, plus or minus 5%. Gas data for 2011 did not include any verification of air contamination in samples. In addition, historical trends of index parameters used to monitor the field were examined for consistency and identification of "outliers." All of the data for NaKCa, quartz, chloride, Cl/B, and excess steam were examined versus time for the wells sampled during 2011. The plots were examined for any trend reversal or increased scatter over the last few years. In general, the trends were consistent and there was no more scatter than during previous years suggesting that the data are of sufficient quality for this analysis.

2. Methodology and analysis

2.1. Brine-liquid data – Temporal and spatial analysis

The 2011 brine chemical data were examined using the temporal and spatial graphs and plots similar to the methodology of Adams (1994-2005). Variations in brine chemistry were examined over space and time, establishing trends in the reservoir and production fluid. In addition, new methods of interpreting the data and characterizing the reservoir conditions which may have produced the observed brine data, which were introduced in the FY2010 were refined in 2011 and are included in this FY2012 Report. Temporal and spatial trends in fluid chemistry were assessed and analyzed as annual shifts. Two-dimensional spatial analysis using mapping software ArcView was used to assess 10-year shifts in certain fluid constituent (Cl, B, etc) concentrations and their ratios (Cl/B) in production brine. Annual changes in chemical geothermometers (quartz, NaKCa) were assessed spatially and temporally. These geothermometers were also compared spatially to gas geothermometers (methane, ammonia).

2.2. Steam NCG data – Temporal and spatial analysis

Since just over half of the production wells at Coso produce only steam (enthalpy is >2600 kJ/kg) (Figure A 1), geochemical evaluation of the field must include steam chemistry. Steam (vapor phase) chemistry is limited to noncondensible gas (NCG), isotopes, and a few semi-volatile components such as boron, which can be measured in steam condensate. At Coso, chemical data available from steam are almost entirely limited to NCG (as opposed to semi-volatile trace elements sometimes monitored in geothermal steam). For this report, the NCG geochemical data were examined to determine what changes have taken place in the gas compositions over time with primary focus on the past 2 years, since the Hay Ranch Injection Project began. Historical data collected since the field started production were examined in more detail previously and can be reviewed in the FY2010 Coso Geochemical Monitoring Report.

A preliminary examination was made using concentrations in parts per million by weight (ppmw), corrected to reservoir conditions. For each well the following were plotted over time: Gas to Steam ratio, NH_3, CH_4, H_2, H_2 / CH_4, H_2 / NH_3, CH_4 / CO_2, NH_3 / Gas, (NH_3+N_2) / (CH_4+CO_2), N_2/Ar, and measured enthalpy. The liquid indices that are normally monitored at Coso, (Cl / B, excess steam, Cl, and geothermometer temperatures) are also included for the two-phase wells.

All the parameters listed above were examined for initial values and the time series were visually evaluated for peaks, troughs, and increases or decreases to the present time. The trends and their associated values are included as an Excel spreadsheet.

Spatial variations in NCG corrected to reservoir conditions, as well as measured gas/steam ratio (G/S) across the field were examined in chemistry trends contoured for all wells, and for steam and brine wells. Gas geothermometers, measured enthalpy,

estimates of reservoir vapor, and certain cation and anion concentration ratios were contoured as well.

2.3. Additional data evaluation

In addition to the previous analyses of brine chemistry, this evaluation focuses on understanding reservoir conditions from geochemical data in four primary areas: Injection, Reservoir Temperatures, Liquid Saturation, and Boiling, with additional focus on the East Flank and West Field.

2.3.1. Injection response

Historically, injection has been primarily spent brine with lesser amounts of condensate and other water. Injection at Coso includes waste brine, steam condensate, and groundwater. Injection response has been evaluated at Coso to date using brine chemistry. Recently, the injection of groundwater from Hay Ranch has increased and in some areas represents the predominant type of injectate.

Tracing injection fluid chemistry seems possible because each type of injectate has unique chemistry (Table 2-1), though all have low NCG. Anions of particular interest included chloride (Cl), boron (B), and the relationship of their relative concentrations to each other (Cl/B). Concentration trends spatially related to injection locations were studied and compared with those trends farther from injection to examine for any indications of injection influence or breakthrough. In addition, lithium (Li) and its relationships to Cl and B were used to more closely analyze the influence of Hay Ranch groundwater injection on that area of the field.

Table 2-1. Average chemical composition of injection fluid types at Coso

Source	Cold Groundwater	Steam Condensate	Waste Brine	
Constituent	Avg Hay Ranch	Avg Sump	Avg Plant	Avg Polyline
Na	115	1624	5455	4264
K	12.8	245.2	956.0	679.8
Ca	83.8	18.3	151.7	103.5
Li	0.10	12.92	37.00	31.72
B	0.2	97.8	241.2	200.8
SiO2	48	574	699	549
As	<0.18	5.78	13.32	10.27
Cl	81	2527	9413	6799
F	0.29	1.93	0.98	1.31
SO4	244	84	91	97
HCO3	296	92	20	26
pH	7.46	7.86	5.03	5.76
TDS	809	4831	15494	11565

Spatial trends of shifting gas to steam ratios (G/S) over time were examined as well, as both groundwater and spent brine or condensate are gas depleted. Gas concentrations proximal to injection areas were compared to those concentrations further from injection as well. Analysis included searching for evidence of influence from degassed injection fluids in the production wells.

2.3.2. Reservoir temperatures

Changes in temperature and enthalpy of fluids in a geothermal reservoir can result from various reservoir processes. For example, breakthrough of cooler injection or natural recharge; or boiling can produce cooling of reservoir fluids. Temperature increases might result from influx of hotter fluids, production of more steam as a result of the preferential permeability of vapor in a fractured feed zone, reservoir drying, or conductive heat transfer from rock to reservoir fluid as fluids flow though different parts of the reservoir to reach a well. The reservoir conditions are evaluated by comparing measured enthalpies and cation geothermometer temperatures for individual wells over time. This method was developed in order to recognize boiling effects in other fields (e.g. Truesdell and Lippman, 1998). In addition, for wells producing both brine and steam, quartz and cation geothermometer temperatures from brine samples are compared with gas geothermometer temperatures for the steam samples collected at the same time. Comparisons of selected gas geothermometer temperatures with quartz and cation geothermometer temperatures can be seen in Figure A 2 through Figure A 12.

For 2011 data, excess enthalpy (measured enthalpy at the surface greater than the enthalpy of liquid at the reservoir temperature) was examined across the entire field in an effort to better understand the evolving temperature trends and the relationships these might have with injection activities. Excess enthalpy calculations were compared with injection trends in an effort to highlight possible patterns.

2.3.3. Boiling, phase segregation, and reservoir liquid saturation

It is well understood that boiling or vaporization can occur as a geothermal reservoir's pressure declines below the gas breakout pressure (the vapor pressure of water plus the pressure of dissolved gas) at reservoir temperatures. Just as it occurs in a producing well in response to the difference between reservoir and wellhead pressure, it can occur within the reservoir as a result of pressure decline related to short-term production or long-term negative net withdrawal.

When a boiling geothermal reservoir isn't recharged with liquid, it typically develops a vapor-dominated zone producing 100% steam. As reservoir pressure declines, if there is some vapor in the reservoir, wells can produce two phase but with more steam than would be expected if liquid at reservoir temperature was flashed ("excess steam"). If reservoir vaporization continues to dryness, the steam becomes superheated. More than half of all Coso wells produce 100% steam and more produce excess steam. In some geothermal reservoirs, production from this steam zone remains constant over many years

as a result of natural and/or artificial (injection) recharge into an underlying deep, liquid-dominated (but connected) part of the reservoir (e.g. Wairaki).

Some areas of the Coso reservoir produce 100% steam but appear to remain on the liquid saturation curve (no superheat in equilibrium with liquid), whereas other highly vaporized areas are hot and possibly dry (very low liquid saturation). In these areas, some excess steam might be related to the addition of heat by conduction, or pressure drop in steam-dominated areas, the steam may become superheated (temperature is above saturation). The addition of injection water to these areas of the reservoir may produce very different results. Because of the importance of evaluating liquid saturation and boiling for reservoir management for long term production from Coso, injection strategy and assessment of reserves, GEOLOGICA has focused on geochemical characterization of boiling and liquid saturation.

The natural partitioning of various parameters between liquid and vapor phase means produced fluid chemistry can help distinguish between excess steam by the addition of heat and excess steam related to phase segregation. In this evaluation, we performed preliminary assessments of the mechanisms of producing excess steam, boiling, and liquid saturation in different parts of the Coso field based on:

- Variations in chloride concentrations in total brine and chloride concentrations in total discharge and corrected to reservoir conditions as well as gas/steam. This methodology was developed by Stephan Arnórsson and others in Iceland (e.g. Arnórsson, 2007)
- Preliminary assessment of gas/steam ratio in the Navy I versus other areas
- Reservoir liquid saturation evaluated using the grid method developed by Franco D'Amore and Alfred Truesdell for both vapor dominated and liquid dominated geothermal systems (e,g. D'Amore and Truesdell, 1983)
- Reservoir liquid saturation evaluated using the WATCH program developed by Iceland Geochemistry group (Arnórsson et al, 1982)

The results of these assessments are discussed below.

2.3.4. Isotopes

Samples were collected to analyze for stable isotopes oxygen-18 ($\delta^{18}O$) and deuterium (δD) again in 2011 in an effort to identify trends in fluid types and establish traceable relationships across the production and injection field. Assessment included comparison of data points from Coso Hot Springs, Hay Ranch water, and previously sampled wells. Isotope ratios were assessed spatially by plotting $\delta^{18}O$ vs. δD grouped by water type and production field area. In addition, stable isotopes were plotted by well over time.

3. Observations, evaluation and discussion

3.1. Temporal and spatial trends

Enthalpy over the last 10 years has increased in the center of the field, while decreasing on the edges. Just over 80% of steam wells field wide have gone superheated with the exception of 4 wells in Navy II area, 3 wells in the southern BLM area and 1 well in the Navy I area. Of the 8 steam wells that are not superheated, 6 are located adjacent to, or on the same well pad as injection wells indicating that injection is likely influencing the potential for superheating where breakthrough is occurring.

When comparing 2001 to 2011 measured enthalpy levels, relative changes have been smaller than observed in the past. Measured enthalpy in 2011 increased by a maximum of less than 700 BTU/lb in only a few wells as compared to more than 1,000 BTU/lb in previous 10-year spans. Additionally, the majority of wells increased in enthalpy by less than 10 BTU/lb over the most recent 10-year span, and 24 wells actually decreased in measured enthalpy during that time, including several in the middle of the field. (Figure A 14).

Trends in changes in reservoir brine chemistry over a 10-year period are less prominent due to the smaller data set associated with the decreasing number of brine-producing wells. Ten-year chloride changes appear to continue to exist in a more west-to-east trend with major decreases in Cl concentration in the west and increases in the east (Figure A 15). These trends may be a result of the closer proximal injection well locations in the eastern part of the field versus the west.

Similar to chloride trends, the 10-year NaKCa geothermometer trends appear to have an east-west correlation. Temperatures appear to warm (~10°C; 50°F) to the east and cool (~15°C: 59°F) toward the west (Figure A 16). However, these changes are small compared to the range across the field (240-380°C; 464-716°F). Quartz geothermometer temperatures also appear to increase in the East Flank and cool in the west and south, but again on the order of 30 to 15°C (86-59°F), respectively, a small change relative to the range across the field of (220-400°C; 428-752°F). Brine geothermometer temperatures from most wells have changed by only a few °C as compared to 2001 data, with a few either decreasing or increasing by as much as 10-30°C (50-86°F) (Figure A 17).

3.2. Chemical indications of injection response

In 2011, injection volumes increased through the east-west oriented center of the field, while injection volumes decreased along the edges. Change in injection volume was relatively minimal (+/-<500,000 kpy (thousands of pounds per well per year)) in most wells, but injection increased in 3 wells (47A-20RD, 47A-8RD, and 24B-8), which increased by more than 1 million total kpy. Well 24B-8 increased in injection volume by 3 million kpy, more than double any other changes from 2010 in any other wells (Figure A 18). Injection into one well (88-1RD) decreased by a little more than 1.5 million kpy. To the south, injection rates also increased in most injection wells, declining in only a

few. Injection rates into the East Flank injection wells was a combination of slight (<500,000 kpy) increases and decreases over 2010 levels.

3.2.1. Chloride

Reservoir chloride concentrations have increased in fluid from many production wells since the late 1980s, most drastically in the southern area (BLM East) (Figure A 19). In comparison to 2001 concentration levels, reservoir chloride in the East Flank, Navy II, and BLM West increased slightly in concentration. Navy I has historically been the only area where reservoir chloride decreased since 1987, as separated by 10-year trends. However between 2010 and 2011, East Flank wells were the only ones to decrease in reservoir Cl concentrations (Figure A 25). Whether increasing or decreasing over time, these trends all appear to generally correlate with changing average injection chloride concentration of a given plant area (Figure A 20 through Figure A 23).

The greatest increase in reservoir Cl concentrations between 2010 and 2011 occurred in the southeastern and northwestern portions of the field. In production fluid near the southern injection wells, increases in Cl have been observed since chemical monitoring began in the late 1980s. Overall, reservoir Cl increased in 8 of the wells measured from 2010 to 2011.

Average Cl concentrations in injected water remained slightly higher than reservoir waters in 2011 (Figure A 24 through Figure A 26). These averages included injection of low-Cl Hay Ranch water, which was periodically added to numerous injected wells across the northern and central portions of the field (Figure A 27). Measured Cl decreased in most of the East Flank wells.

Contour maps of Cl concentrations in injection water, produced brine and calculated reservoir fluid, and overlain reservoir chloride and injection Cl concentrations indicate that high injection chloride and high reservoir chloride correlate spatially in the southeast (BLME) (Figure A 28 through Figure A 30).

This year, chloride concentrations were corrected using two methods in order to confirm results. Figure A 28 shows reservoir chloride corrections using the more traditional steam fraction and excess steam method, while Figure A 29 corrects Cl to reservoir conditions using the WATCH method employing sampling conditions (Sep P/T, discharge enthalpy, etc) and estimated reservoir temperature based on quartz geothermometer. As the figures show, the two different methods result in similar values, verifying both methods are effective at producing reservoir conditions.

In BLME, where the majority of injection occurred, the Cl concentration of reservoir brine (produced brine corrected to reservoir conditions) currently appears to be in between low and high Cl concentration injectate (**Error! Reference source not found.**), aking it difficult to attribute increases in corrected brine Cl to injection. Since chloride increases are observed at the beginning of production, in the months prior to initiating

injection (mid-1989), it cannot be attributed solely to injection. However, the Cl concentration trends in injection fluid tend to be similar to those of reservoir Cl field wide: where production fluid is high in Cl, injection is also high. This can be partially explained by the fact that most injection at Coso has been waste brine that has been injected within the plant area where it was produced. This suggests there may be some additional processes contributing to the increase in Cl, such as reservoir boiling or the influx of higher salinity brines.

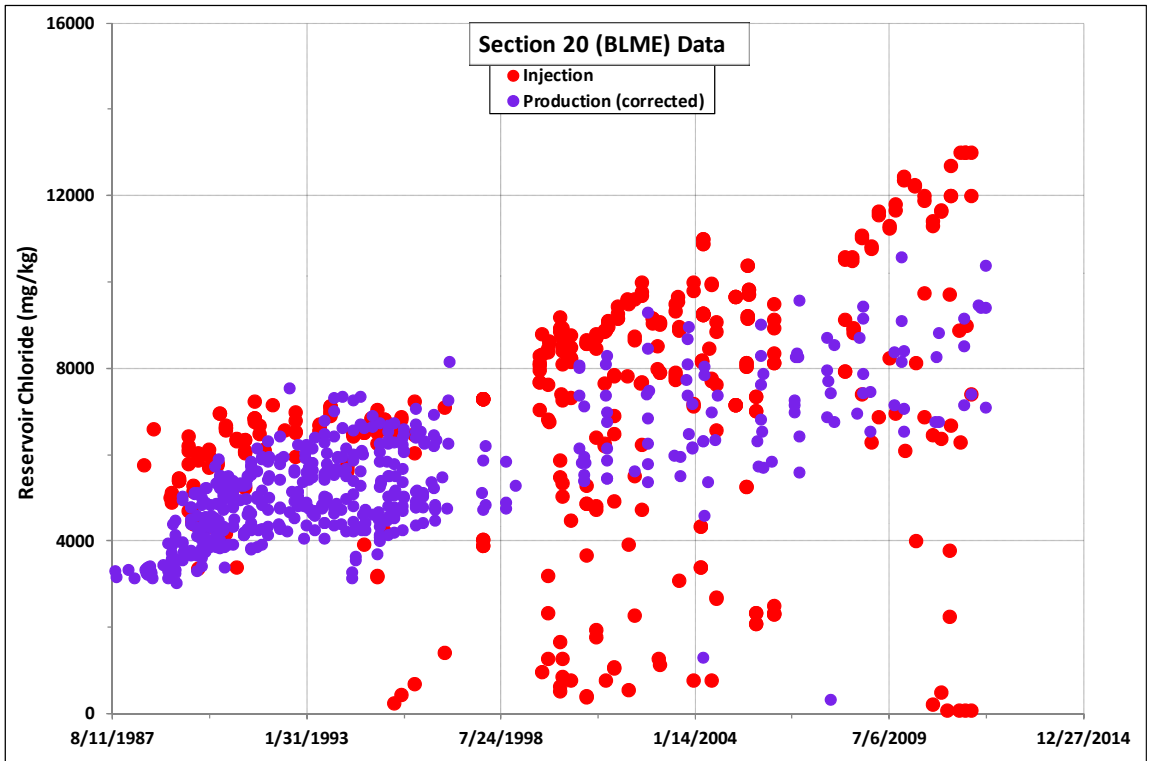

Figure 3-1. Comparison of chloride in injectate and reservoir brine in BLME. Historical injection data is before the Hay Ranch injection project.

In 2011, the average chloride concentration of injectate was 4,826 ppm and the average concentration of produced brine was 7,683 ppm, which, when corrected to reservoir conditions, indicates an average reservoir brine concentration of 5,390 ppm. However, in reservoir fluid in the southern injection area, Cl concentrations ranged from just over 3,500 ppm to just over 9,000 ppm. In reservoir liquid, the concentration of Cl in injection fluids in this area varies from 4,000 to 13,000 ppm depending on the source of the injectate.

In the East Flank, Cl concentration of reservoir liquid in wells producing brine ranged from 2,700 to 9,700 ppm in 2011. Cl concentrations were lower in several of the wells (26A-9, 38C-9, 38D-9 and 42A-9) sampled in 2011. This wide range suggests both permeability barriers and multiple fluid sources, which may include different sources of injection water, different influx, brine condensate, or initial variations in reservoir Cl.

Reservoir fluids supplying wells in the North of the field (Navy I) maintained the lowest concentration of Cl, ranging from 1,577 to 2,283 ppm. Chloride concentrations in fluid injected on the north side of the field are around 75 to 3,000 ppm depending on the injectate source (condensate, Hay Ranch, waste brine, etc.). Hay Ranch water containing less than 100 ppm Cl was injected into several Navy I injection wells in all four quarters of 2011. However, because condensate and Hay Ranch waters are both low in terms of Cl and B concentration (compared to waste brine for example), tracing reservoir response to Hay Ranch water may be more difficult or impossible in the Navy I area. Chloride concentrations in the reservoir and injection rates remained mostly stable in the north, with very little change (<10%) from 2010. The north end of the field has fewer injection wells with less volume, and wells sampled in 2011 in the north tended to be farther from injection wells than wells sampled in other parts of the field.

Chloride decreases in production fluid might be related to the influx of low chloride groundwater or injectate (Hay Ranch) or steam condensate. Where chloride increases correlate with lower enthalpies and low gas, it would be expected that the source of the chloride increase was injectate of spent brine. The spatial correlation of low enthalpy and chloride increases (Figure A 31) is most distinct in the southeast part of the field and therefore it appears likely that chloride is tracking injection in this area. However, since the current maximum chloride in reservoir fluids in this area remains greater than the proximal injectate (Figure A 30), processes other than mixing of reservoir liquid and injectate (such as boiling) are occurring.

In summary, there appear to be multiple processes affecting chloride concentrations in the Coso reservoir. Chloride increases in production fluid might be related to in-situ boiling of reservoir fluid or breakthrough of high-chloride injectate or other high-Cl reservoir brine. Production of 100% steam wells and vapor saturation evaluation suggest that reservoir boiling occurs. The effects of boiling on Cl are discussed below.

3.2.2. Chloride / Boron

Because of their conservative character, chloride/boron (Cl/B) ratios in geothermal reservoir liquids are typically constant. However, boron has a higher volatility and is concentrated in steam (e.g. Adams, 2002; 2004). Therefore, Cl/B ratios can change in wells with higher temperature boiling as seen in excess steam wells or wells that are affected by condensate injection. At Coso, Cl/B ratios in produced brine display spatial variations, some of which were observed in the initial production in the 1980s. Historically, the Cl/B ratio in produced brine have roughly correlated with Cl/B in injection fluid which is primarily waste brine (e.g. 2010, Figure A 37). In 2011, the relationships reversed, primarily because the Cl/B of injectate changed (Figure 3-2; Figure A 32 through Figure A 36).

In 2011, as previously, most wells in the north and east that produce brine had Cl/B ratios ranging from 30 to 40, while wells to the south tended to have ratios in the 40 to 60 range. In 2011, the lowest Cl/B ratios were found in brine from the northern portion of the field and northern East Flank. The highest ratios ranging from 71 to 80 were

clustered closest to the wells injecting the highest volumes in the southern portion of the field. In the East Flank, the lowest ratios occurred around the injection Wells 34-9RD2 and 51B-16, although these wells had low injection volumes in 2011. One well (26A-9) in the northern portion of the East Flank had the lowest ratio (7-10); however, this well is producing very little brine (~85% steam), has very low Cl concentrations, and appears to be producing condensate.

Despite these variations, the liquid Cl/B ratio of produced brine in 2011 is relatively consistent (approximately 40) with previous years compared to the change in Cl/B in injection fluids (Figure A 36). The Cl/B ratios in average injection fluids in 2011 ranged from 25 to 150, reflecting a wide range of sources of injection water including the high Cl/B ratio Hay Ranch water. Historically, waste brine has had the highest Cl/B ratio because as it was boiled, boron is preferentially lost during boiling. In contrast, steam condensate is likely to have the lowest ratio as boron preferentially partitions into steam. The observed variation in Cl/B in fluids produced near injection wells has been consistent with the Cl/B injection of brine in the southern part of the field near BLMW. Low Cl/B ratios in two-phase wells may also reflect condensate injection in the Navy I area or production of steam condensate (**Figure A 40**). During 2011, injection of Hay Ranch water in Navy I and the East Flank changed the relationship between Cl/B in injectate and produced brine (Table 3-1; Figure A 36 and Figure A 37).

Table 3-1. Average Cl/B ratio of injection fluids at Coso

	Cold Groundwater	Steam Condensate	Waste Brine	
Source	Avg Hay Ranch	Avg Sump	Avg Plant	Avg Polyline
Inejction Cl/B	338.00	25.85	39.03	33.86

Historically, Cl/B ranges in injection fluids have been within the range of production wells within the same power plant area, which may limit any visible influence of injection fluid on production Cl/B ratios (**Figure A 38** through **Figure A 42**). However, the addition of high Cl/B-ratio Hay Ranch water to the system in some areas, as discussed above, may have future effects on production Cl/B ratios. While possible trends of increased Cl/B can be seen in some select wells such as 83B-16, 51-16, 52-7, and 38D-9, since the beginning of Hay Ranch injection, larger field-wide trends are not yet visible (**Figure A 38** and **Figure A 40**). Future investigation should include closer examination of Cl/B trends over time, particularly in those wells with proximal relation to Hay Ranch injection wells.

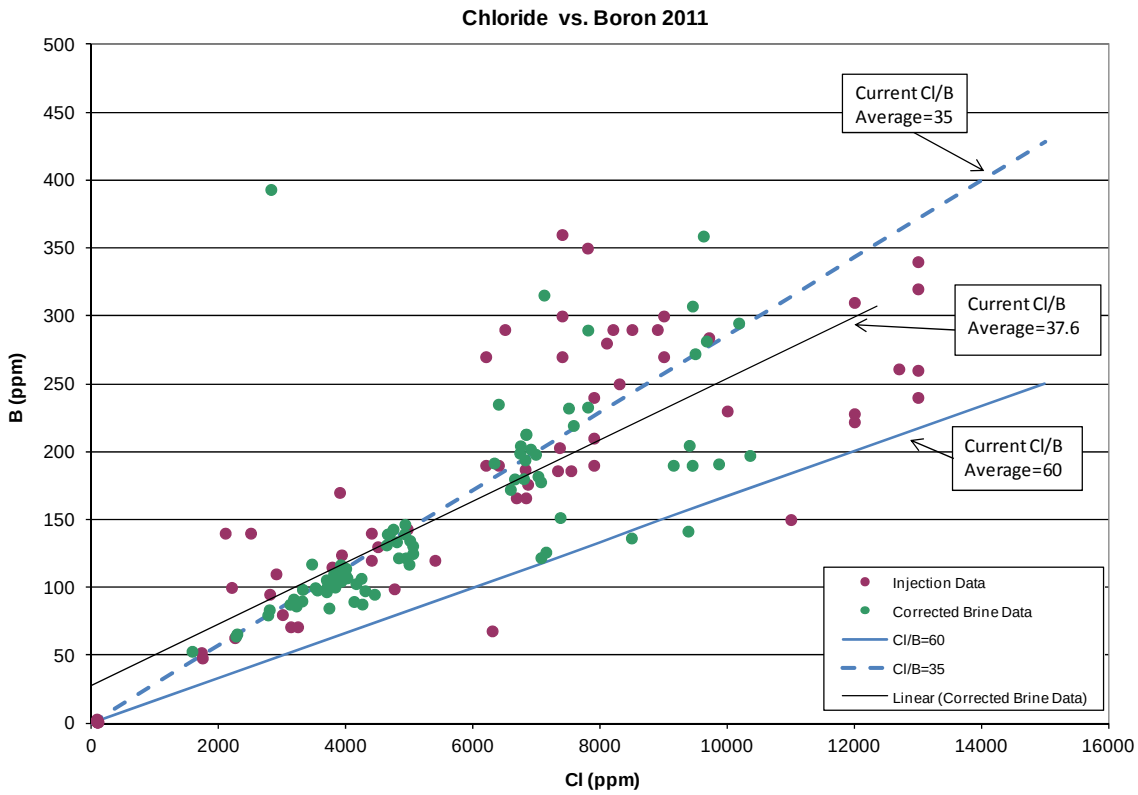

Figure 3-2. Cl/B in 2011-produced reservoir fluids and injection (all injection fluids)

3.2.3. Gas/Steam and gas composition

As the volatile component of the geothermal reservoir fluid, noncondensible gas (NCG) partitions into the steam phase either at the separator upon discharge or in the reservoir if a vapor phase develops there. Because almost all NCGs partition into the steam phase after a small amount (<3%) of boiling, boiled reservoir brine is subsequently degassed. In order to maintain constant NCG levels in produced steam in a two-phase geothermal reservoir, the source of the steam must be previously unboiled brine. For NCG concentrations (as gas/steam (G/S) in parts per million by weight (ppmw) in produced steam) to increase, either: (1) steam is condensed before discharge, (2) produced steam is exotic to the area (not in equilibrium with brine), (3) brine is exotic to the area and still gas-saturated, or (4) steam is generated from a much smaller amount of boiling (cooling). Declines in G/S indicate either production of steam from boiling of previously boiled brine (or injectate whether brine, groundwater or condensate) or boiling significantly larger percentage of brine.

Measured G/S ratios varied from 6,000 ppmw to over 77,000 ppmw across the Coso field (Figure A 43) in 2011. Noncondensible gas/steam changed minimally (+/- <4,000 ppmw) since 2010 in most of the field, with the exception of a couple of areas in the south, East Flank and middle of the field (Figure A 44). In the North, NCG concentration changes from 2010 to 2011 ranged anywhere from negligible to ±<5000

ppmw. The largest decrease in measured G/S change between 2010 and 2011 occurred in the East Flank, especially in well 83B-16, which decreased from 22,250 ppmw to 14,450 ppmw. The East Flank also recorded the second largest 1-year increase in well 26A-9 of 15,878 ppmw to nearly 51,000 ppmw. G/S in steam produced from 37B-17 increased the most; from ~28,000 ppmw to 48,364 ppmw.

Comparing the current year to 10 years ago (2011 compared to 2001; (Figure A 13)), the measured noncondensible gas (gas/steam ratio) in produced steam from the Coso field has increased mostly in the middle of the field, in the central steam-dominated region of Navy I and in one well, 35-B20, by at least 7,500-15,000 ppm, to as high as nearly 75,000 ppm, with a few areas of decrease along the flanks. In contrast, four wells along the southern boundary of the field, one well in near the middle, four wells in the north, and five in the East Flank appear to have decreased NCG compared to 2001.

Several historical trends of measured NCG data (gas/steam) from 1987-2011 vary between areas. Wells in Navy I and Navy II have shown the most consistent increases in the field. Most notably, since 1999 the wells in these areas increased in measured G/S indicating that either (1) steam is condensed before discharge, (2) the areas near the edge of the field are seeing an influx of exotic vapor or brine, or (3) the measured steam is generated from a much smaller amount of boiling (cooling). Measured NCG in production wells in the East Flank and BLME has been sporadic but has generally remained constant over time. Gas/steam in BLMW wells is mostly constant with G/S increases observed in a few wells. This indicates that the source of steam in these areas is likely previously unboiled brine (Figure A 68 through Figure A 72).

In order to evaluate whether these historical trends might be related to reservoir conditions, the measured gas/steam was corrected to concentrations of NCG in reservoir fluids. Concentrations of NCG dissolved in reservoir liquid (steam samples corrected to reservoir conditions based on enthalpy and sampling conditions) had a much more consistent pattern in 2011 than G/S. In 2011, NCG concentrations were consistently low in the center and north of the field and higher along the edges, particularly in the East Flank and south. Concentrations of NCG since start-up have increased slightly in the Navy I reservoir (Figure A 43 and **Figure A 44**), with a few wells, 47-8, 47A-8 and 66-8 showing strong increases since 2005 (Figure A 71). NCG concentrations in the East Flank appear to have decreased since about 2008, with the exception of 26-9 (Figure A 75). BLME and BLMW show both decreases and increases, but BLME reservoir appears to show an overall decrease in NCG (Figure A 73 and Figure A 74). These values show high scatter, probably because they are calculated based on enthalpy measurements, which also show variability.

The composition of NCG at Coso is dominated by CO_2, but it appears that concentrations of other gases are buffered by gas reactions (Figure A 65 through Figure A 67). Trends in H_2S relative to CO_2, (H_2S/CO_2) may reflect variations in reservoir conditions because H_2S is more soluble than CO_2, and participates in different reactions and therefore variations can reflect differences in reservoir saturation. Although variations over time

do not appear significant (Figure A 83), the range in H_2S/CO_2 across the field from a high of 0.04 in the East Flank to lows of <0.005 in the center are significant (Figure A 65).

The spatial distributions of H_2S/CO_2, H_2/CO_2, and CH_4/CO_2 across the field (Figure A 65 through Figure A 67) show a distinctive pattern of highs at the outer edges (particularly in the southwest, north, and East Flank) and lows in the center and southeastern parts of the field. Whereas H_2/CO_2 is consistent across the field except for slightly higher values in the east and northeast, especially one well (83B-16), CH_4/CO_2 is the opposite and shows highs in the west and south. H_2S/CO_2 shows broader areas of high concentration in areas at the edges of the field where wells produce brine and lows in the central steam field, consistent with the more liquid-soluble character of H_2S.

3.2.4. Isotopes

Review of isotope data from 2011 compared to data points from Coso Hot Springs, Hay Ranch water, and previously sampled wells suggests that the 2011 results fall within the range of previously sampled wells (Figure 3-3). The temperature and degree (fraction) of boiling will affect the stable isotopic composition of injection derived steam. As shown in Figure 3-3, the isotopic composition of steam derived from Hay Ranch water will depend on the temperature of boiling. If partial boiling occurs at approximately 220°C (428°F), steam may be indistinguishable, but at lower or higher boiling temperatures or partial boiling temperatures, the isotopic composition of Hay Ranch-derived injection should be discernible in Coso steam. In addition, the overall trend in isotope data from a geothermal field often identifies the boiling temperature. The 2011 data suggest that boiling occurs in the Coso reservoir at approximately 190°C.

If Hay Ranch injectate boils and the resultant steam mixes with reservoir steam, the total isotopic composition of the resultant steam should become lighter in oxygen-18 (more negative) and may not change the deuterium a great deal, depending on the boiling temperature. If the Hay Ranch injectate mixes with reservoir brine and then boils, both oxygen-18 and deuterium might become more negative depending on the degree and temperature of boiling (Figure 3-4; Figure A 84 through Figure A 97 show graphical representation). To date, no significant trends in isotopes of produced fluids can be attributed to injection of Hay Ranch water.

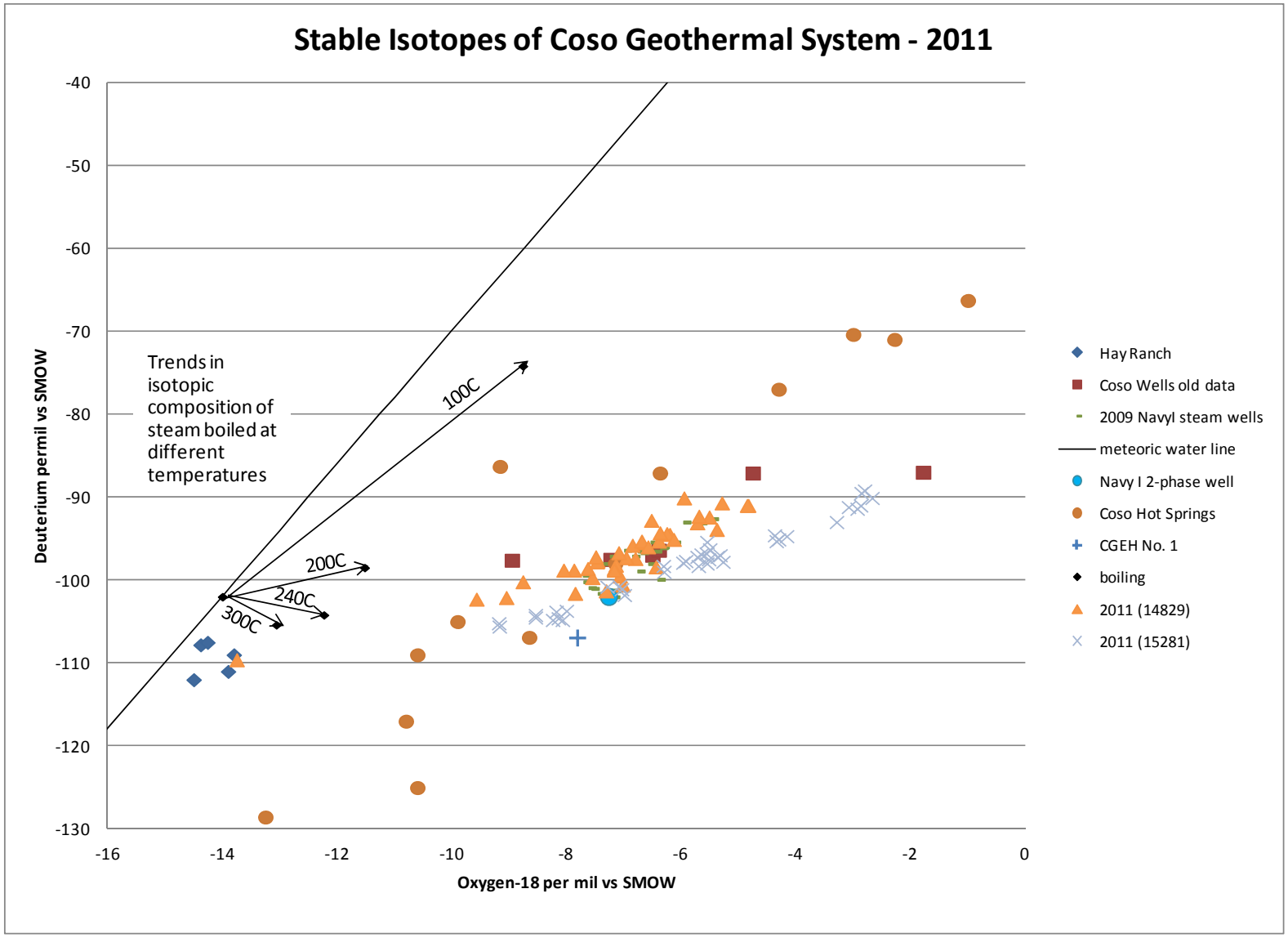

Figure 3-3. Stable isotope data of the Coso Geothermal System in 2011

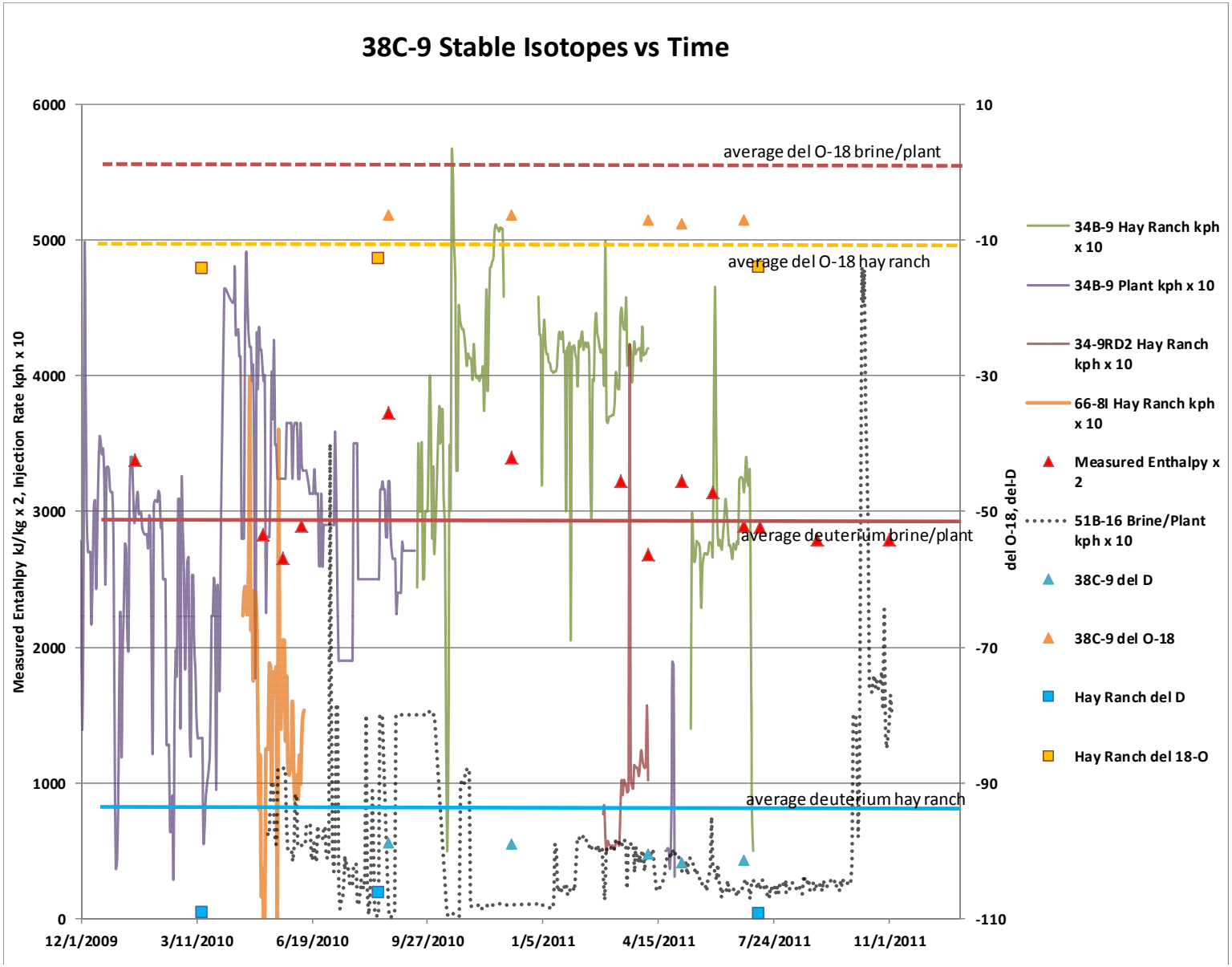

Figure 3-4. 38C-9 Trends in Oxygen-18 and Deuterium with injection over time

3.3. Temperature

Reservoir temperatures are monitored using chemical geothermometers as well as downhole measurements. Geothermometers are based on chemical concentrations in geothermal fluids that are based on temperature-dependent equilibrium reactions with reservoir rocks (minerals). Since the host rock fluid sources and temperatures differ between geothermal fields, the applicability and accuracy of geothermometers also differ. Because some geothermometers equilibrate more rapidly (silica) than others, and some are focused on the vapor phase (gas geothermometers) or the liquid phase (silica and sodium/potassium (Na/K)), differences can reflect phase differentiation in the reservoir and temperature changes related to reservoir conditions that are unrelated to injection breakthrough, such as boiling.

3.3.1. NaKCa geothermometers

The sodium-potassium-calcium (NaKCa) geothermometer calculations reflect reservoir temperatures from areas of the reservoir that produce brine. Temperatures estimated from the NaKCa geothermometer are highest (>280°C; 536°F) in the East Flank (e.g. 83A&B-16; 42B-16; 38D-9; 26A-9 (270-280°C; 518-536°F)) and west-southwest part of the field (e.g. 16 A&B-20 (270°C; 518°F) and 33-19 (280°C; 536°F). The lowest temperatures (<260°C; 500°F) occur in the center and southern part of the field where brine is still produced from 35B-20, adjacent to BLME injection to 52-20, 16-20, 65A-18 and 33-7.

NaKCa geothermometers remained mostly consistent across the field in 2011 with only slight (+/-<10°C; 50°F) shifts compared to 2010 calculations (Figure A 2 through Figure A 4) except 26A-9. Geothermometry suggests about half the wells cooled by approximately 0-9°C (32-48°F), while the other half warmed by 1-10°C (34-50°F). While most wells in the East Flank cooled, one well (26A-9), increased by more than 60°C (140°F). Wells in the center and some in the southeast of the field tended to cool, while wells in the southwest and north increased by a few degrees. Data collected in 2011 returned to the previous trends of NaKCa geothermometer calculations, which had previously been trending mostly down in the East Flank, while it trended mostly up in the south. Like previous years the trend remained mostly stable in the north.

3.3.2. Quartz geothermometers

The silica concentration of produced brine is used to estimate reservoir temperature based on the temperature-sensitive reaction between water and quartz in reservoir rocks. It is a relatively fast reaction and therefore is considered the best chemical tracer of current reservoir liquid temperatures. Temperatures estimated from the quartz geothermometer are highest (>280°C; 536°F) in the East Flank (e.g. 83A&B-16; 42A-16; 38 B&D-9; 26A-9 (270-280°C; 518-536°F)) and west-southwest part of the field (e.g. 16 A&B-20 (270°C; 518°F) and 33-19 (280°C; 536°F). The lowest temperature (~225°C; 437°F) is indicated in brine from 35B-20, adjacent to BLME injection. The quartz geothermometer suggests a much smaller area with brine temperatures less than 260°C (500°F) compared

to NaKCa geothermometers, and only in the southern part of the field, relative to the slower reacting cation (NaKCa) geothermometer suggesting that the center of the field may be drawing in hotter fluids.

The quartz geothermometers remained mostly stable across the field (Figure A 5 through Figure A 7). In the north, calculated temperatures for one well (68-6) increased by ~7°C (~45°F), while the other (33-7) decreased by just over 10°C (50°F). In the East Flank, temperatures estimated from the quartz geothermometer increased by 1-20°C (34-68°F) in most wells. The highest increase in the field occurred in 26A-9 at nearly 55°C (131°F), consistent with the large increase in reservoir liquid temperature indicated by the NaKCa geothermometer, and suggesting that the feed zone in 26A-9 is hotter. In the south part of the field, most wells remained stable, with a few wells shifting a few degrees (±<10°C (50°F)). The largest decrease was in the center of the field (65A-18) at 10°C (50°F).

Typically brine is injected in the East Flank directly from the EF Separator at 165°C (330°F). Elsewhere brine injection occurs at lower temperatures related to the power plant LP flash pressure. In contrast, Hay Ranch water is injected at approximately ambient conditions (average 20°C, 68°F). Because there is a significant temperature difference, Hay Ranch injection might cool reservoir fluid temperatures. Because the quartz geothermometer is relatively quick to respond, silica concentrations (and quartz geothermometer temperatures) might reflect this cooling. Lack of significant changes in silica from previous years to 2011 (with the few noted exceptions) do not indicate significant cooling related to Hay Ranch injection to date, but monitoring should continue to assess this possible impact on reservoir temperature.

3.3.3. Gas geothermometers

Estimated temperatures from methane (CH_4) and ammonia (NH_3) gas geothermometers were relatively consistent again in 2011 (Figure A 8, Figure A 9). Contour trends were similar to 2010 with respect to spatial distribution. However, in 2011 the hottest reservoir temperatures suggested by gas geothermometers were in the East Flank, followed then by the historically high southwestern (BLMW) portion of the field. The hottest gas NH_3 geothermometers were calculated at 398°C (748°F), slightly cooler than the maximum 420°C (788°F) calculated last year. The highest CH_4 geothermometers were calculated at 426°C (800°F), similar to 2010. In addition, steam from parts of the center of the field appear to be >400°C (750°F), which is not observed in the brine geothermometers as no brine is produced from this zone. The coolest gas geothermometer temperatures were in areas with significant injection flow in the very northern part of the field and the southeast.

3.3.4. Gas vs. Cation geothermometers

In the event that a well is still producing enough of both brine and steam to sample, cation and gas geothermometer calculations were compared to examine trends over time. Wells containing less than 10% excess steam as well as many wells containing 20-80%

excess steam were sampled for both gas and brine analysis. Methane and cation geothermometers as well as enthalpy measurements were plotted over time (Figure A 10 through Figure A 12). Trends remained mostly stable in 2011. As previous analysis has shown, cation geothermometers remained consistent and flat, while methane geothermometers tended to correspond with changes in measured enthalpy. When enthalpy increased, so did gas geothermometers, and vice versa. The implications of these trends reaffirm that as reservoir temperatures increase and the reservoir begins to dry out and shift to steam dominated, gas geothermometers more accurately depict dynamic reservoir conditions.

3.3.5. Temperature summary

The most dynamic temperature data set collected at Coso is the enthalpy measured at the surface (wellhead or separator). In areas such as the East Flank, the measured enthalpy is primarily controlled by the amount of excess steam present whereas in the saturated steam wells of the central field, the measured enthalpy is controlled by WHP. In liquid dominated areas, the measured enthalpy is controlled by the reservoir temperatures. Therefore, in order to evaluate reservoir temperatures, GEOLOGICA reviewed trends in parameters other than surface enthalpy.

3.3.6. Measured temperatures

Where available, static downhole temperatures measured at the main fluid entry level are higher than temperatures estimated from liquid geothermometers but in the same range as gas geothermometers. They range from 265-330°C (510-625°F) in East Flank wells and 238-316°C (460-600°F) in west field wells. These temperatures probably reflect the rock temperatures. Dynamic (flowing) surveys also indicate lower temperatures, but total discharge enthalpy measured at the surface correlates to static measured temperatures (Figure 3-5). This correlation suggests that excess steam is added to the total fluid discharge when rock temperatures remain high enough to boil reservoir liquid. If reservoir fluid is already steam, rock can add heat, creating superheated steam at the surface.

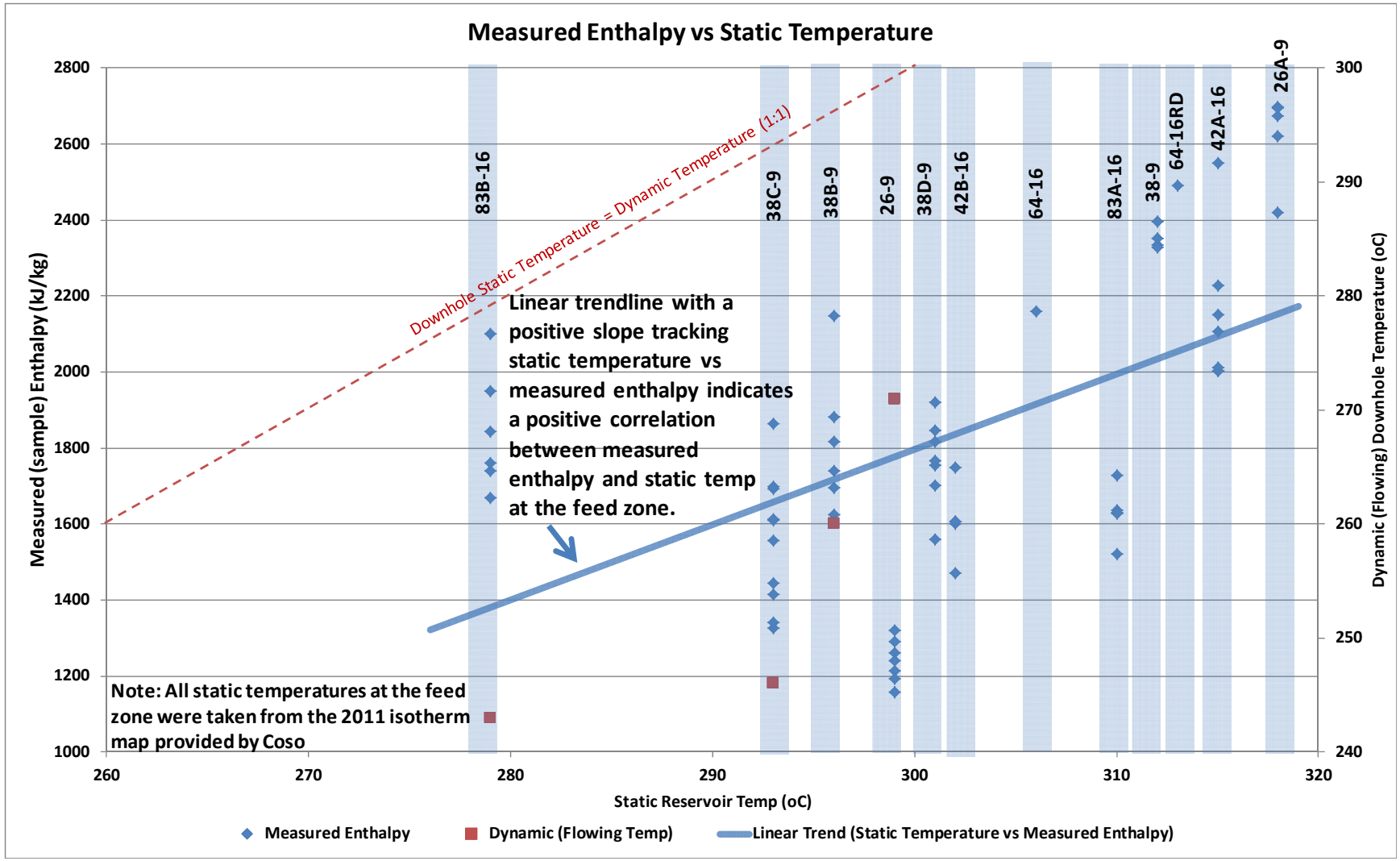

Figure 3-5. Downhole static reservoir temperature (°C) versus measured enthalpy (kJ/kg) (left Y-axis) and downhole dynamic temperatures (°C) (right Y-axis)

3.4. Steam wells and boiling

3.4.1. Steam wells

In 2011, the phase of produced fluid (steam or steam+brine or brine) remained mostly consistent with historical trends. As in years past, wells producing 100% steam were confined to the center of the wellfield. It appears only a few wells have shifted their production phase in the past year. In the south and north, a few wells shifted to full steam, while a few shifted away from full steam to 2-phase; leaving little relative net change (Figure A 1).

3.4.2. Measured enthalpy

In 2011, measured enthalpy remained mostly consistent with the previous year. The highest enthalpy area remains the north central part of the field, dominated by the highest density of 100% steam wells with another small high in the south (Figure A 102). The lowest enthalpy areas occur on the edges of known production, most notably in the southeast (16-20, 16B-20, 24-20RD, and 52-20); northwest (78B-6, 33-7, and 43A-7); west (58A-18) and East Flank (26-9, 42B-16, and 83B-16). Few injection wells are in the middle of the field. When compared to measured enthalpy from 2011, changes are typically less than 10% except for an enthalpy increase in the center of Navy II near 72-18 and 72-A18 (which is now low pressure production) and an increase in 43-7.

Several historical trends have been observed from analysis of enthalpy data collected from 1987-2011. A majority of the wells across the Coso field show isolated trends over short periods of time but generally exhibit gradual increases in enthalpy since the beginning of collection in 1987 to 2011. The most notable increases are seen in Navy I, Navy II, and BLMW between 1996 and 1999. This three-year period marks large increases in enthalpy in various wells in these three sections. These sharp increases in enthalpy, along with the general increase across the field can most likely be attributed to an increased amount of reservoir boiling and thus higher reservoir steam saturation and higher steam fraction at discharge (Figure A 68 through Figure A 72).

4. Boiling, phase segregation, and liquid saturation

Areas where reservoir boiling is efficient or liquid saturation is low may prove to be good areas for in-field injection and, in particular, may have higher potential for generating injection-derived steam (IDS). Areas of vapor-dominated geothermal reservoirs producing super-heated steam, where that steam is derived from the addition of heat to dry steam in the reservoir (as opposed to reducing pressurized dry steam), produce high higher amounts of IDS. While Coso is not a vapor-dominated reservoir, there may be areas sufficiently hot and dry where similar conditions exist. In an attempt to understand variations in boiling across the Coso field, we have focused on evaluating the sources and conditions of excess steam and reservoir vapor from the relationship between gas concentrations within the field, enthalpy, and chloride in produced fluids.

Reservoir vaporization is clearly widespread at Coso: just over half of the wells produce only steam and all but a handful produce more steam than could be generated by boiling reservoir brine at the separation pressure, known as "excess steam." This "excess steam" can be produced in several ways. Good target areas for producing IDS are primarily those areas that produce super-heated steam by adding heat to dry steam on its path from the reservoir to the well. The mechanism for generation of excess steam and super-heated steam can affect both the produced brine and steam chemistry.

4.1. Boiling model

Previously, we created a simplified model that generates differences in noncondensible gas (NCG) concentrations in steam based on different amounts of boiling of a reservoir liquid that was equivalent to that produced (steam + brine recombined) in 100% brine wells. Assuming that NCG partitions entirely into the steam and that boiling occurs in a single stage allows us to create a simplified model for a qualitative evaluation of G/S distribution and boiling within the Coso field. Using G/S data from two-phase wells that produce no excess steam (reservoir fluid is liquid), the average NCG concentration in the reservoir brine is approximately 3400 ppm by weight (ppmw). In wells that produce 100% steam (reservoir fluid is steam), G/S in produced fluid ranges from ≈10,000 to ≈110,000 ppmw but is typically 15,000-30,000 in the central steam zone.

Variation of G/S in 100% steam wells can be produced by boiling from <0.05% to approximately 0.4% brine with reservoir NCG averaging 3400 ppmw. Steam from wells producing no excess steam produce a steam fraction of 0.17-0.31 at separation pressure with NCG concentrations ranged from 6,000 to 27,000 ppmw. The overlap between the concentrations of steam in 100% steam wells and steam produced from reservoir liquid suggests that in some areas (Navy I), the steam and liquid in the reservoir are in equilibrium. These observations also suggest that a higher degree of boiling (15-40%) occurs in the Navy I area than in the BLM area (<10%), the reservoir brine has a different gas concentration or the source of reservoir vapor is different (not in equilibrium with brine).

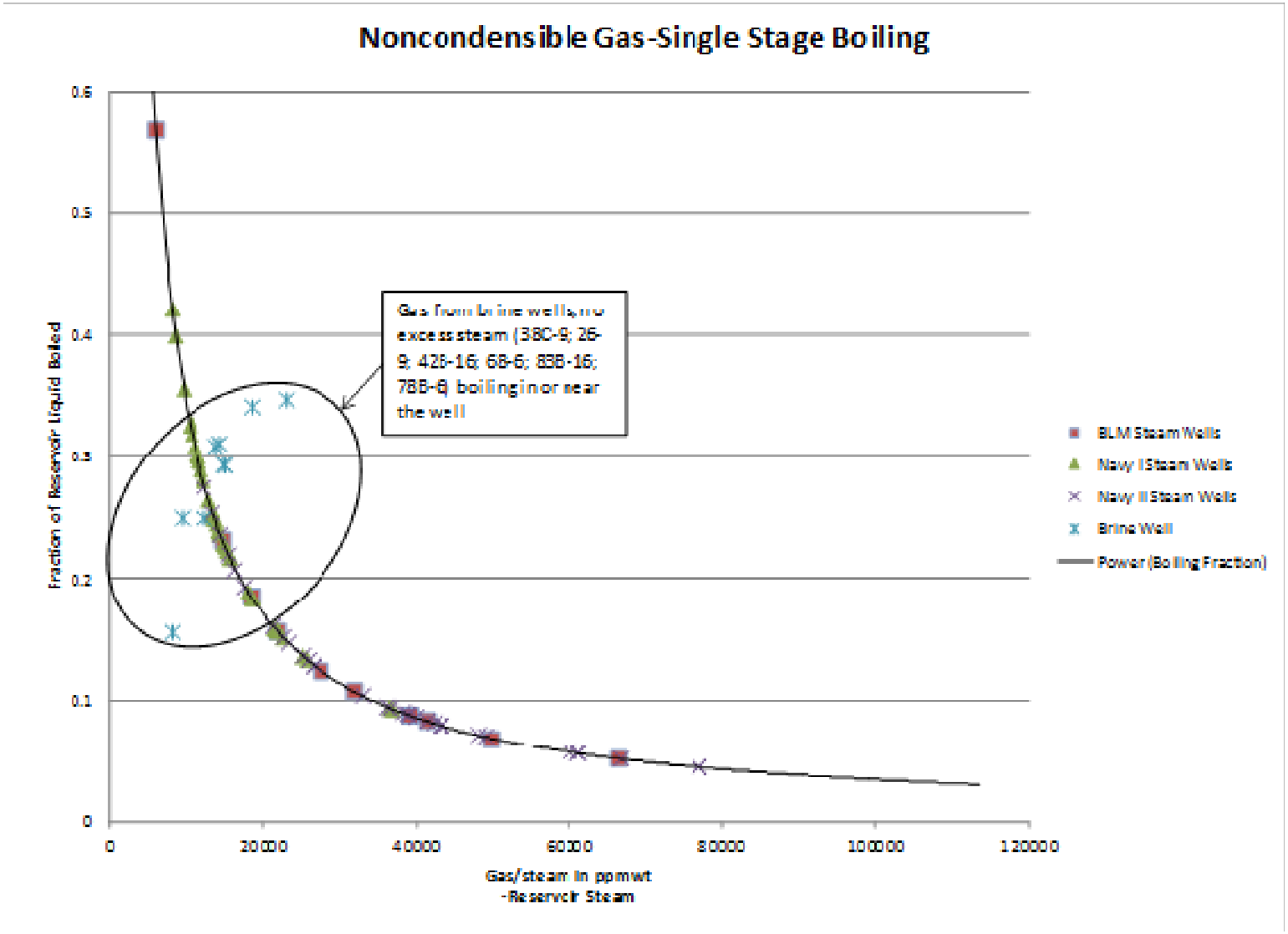

Figure 4-1. Changes in G/S derived from variable fraction of single-stage boiling of reservoir liquid equivalent to brine wells

Since steam produced at Coso has not displayed a significant decline in G/S, continuous or additional boiling of brine does not seem to be the source of steam in the vapor-dominated portions of the field. It appears more likely that the source of steam, particularly in the Navy I area, is boiling of brine recharge or newly-accessed brine, which is boiled in a single stage in the vicinity of 15-20% from a similar reservoir fluid.

4.2. Dynamic versus static temperatures

Dynamic (flowing) and static downhole temperature surveys (provided by COC and available for a limited number of wells) indicate a significant difference in temperature between flowing and static conditions. In addition, vaporization indicated by applying the grid evaluation to gas data, although indicating a wide range of reservoir vapor fractions, suggests that in the area where excess steam is observed at the wellhead, reservoir vapor averages 5-20%.

4.3. Y-values

"Y" values are a chemical-based estimation of steam derived from reservoir vapor relative to boiled reservoir liquid based on gas chemistry of the temperature-dependent methane-breakdown (Fischer-Tropsch) and hydrogen-hydrogen-sulfide reaction. Calculated "y" values maintained a relatively consistent distribution as with previous years. However, y-values have continuously increased in source wells (Figure 4-2, Figure 4-3, Figure A 108). There appears to be correlation between increasing measured enthalpy and increased y-values.

Y-values correlate with reservoir vapor. The Y-values at Coso calculated from the Y-grid are typically <0.25, suggesting that although vapor present is in equilibrium with liquid, there are large areas of boiling within the reservoir where the vapor phase may be dominant. These areas of high vapor saturation appear to have lower reservoir temperatures.

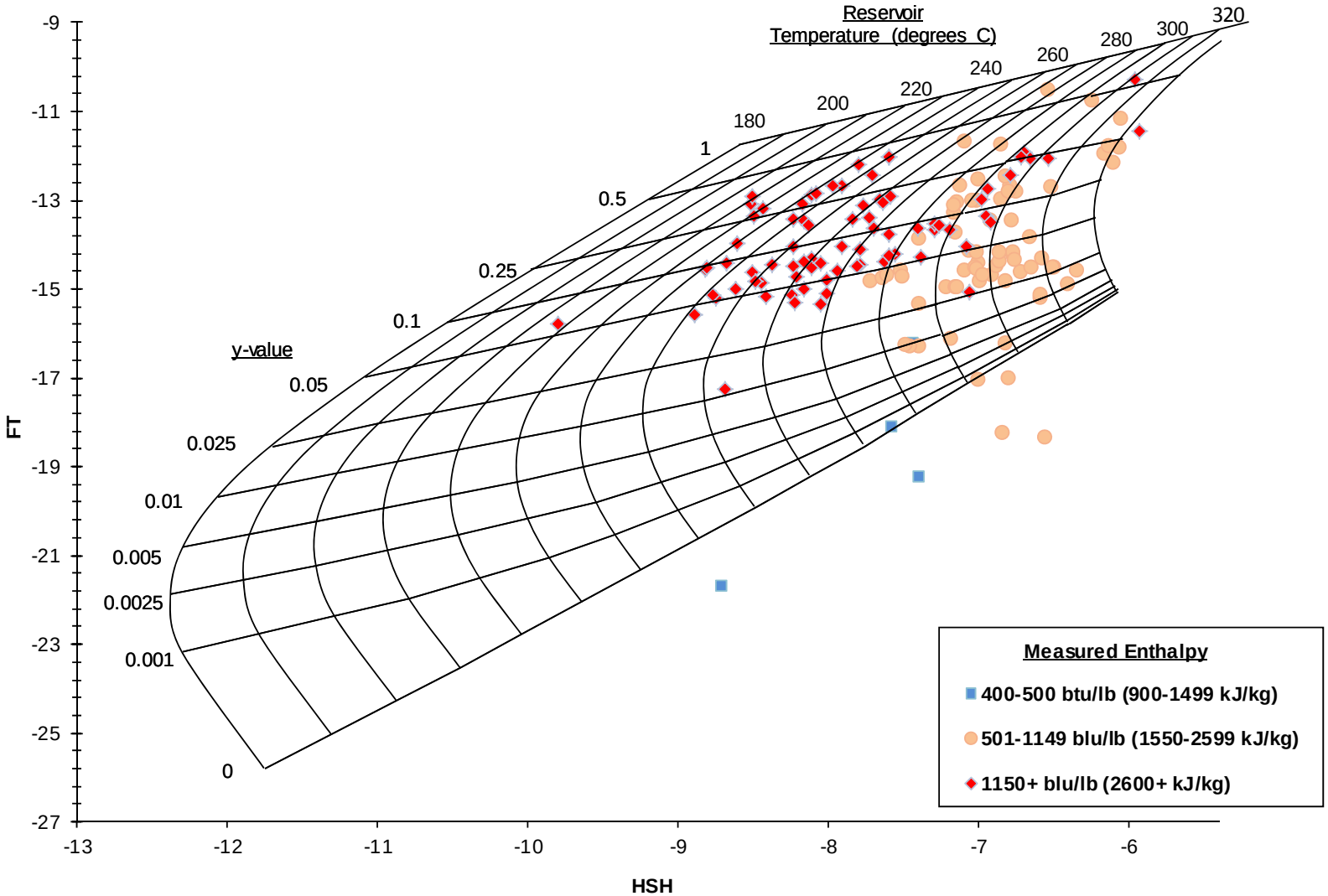

Figure 4-2. Grid Y-values for 2011 based on gas equilibrium FT (CH_4 breakdown to CO_2 and H_2) and HSH (H_2-H_2S reaction)

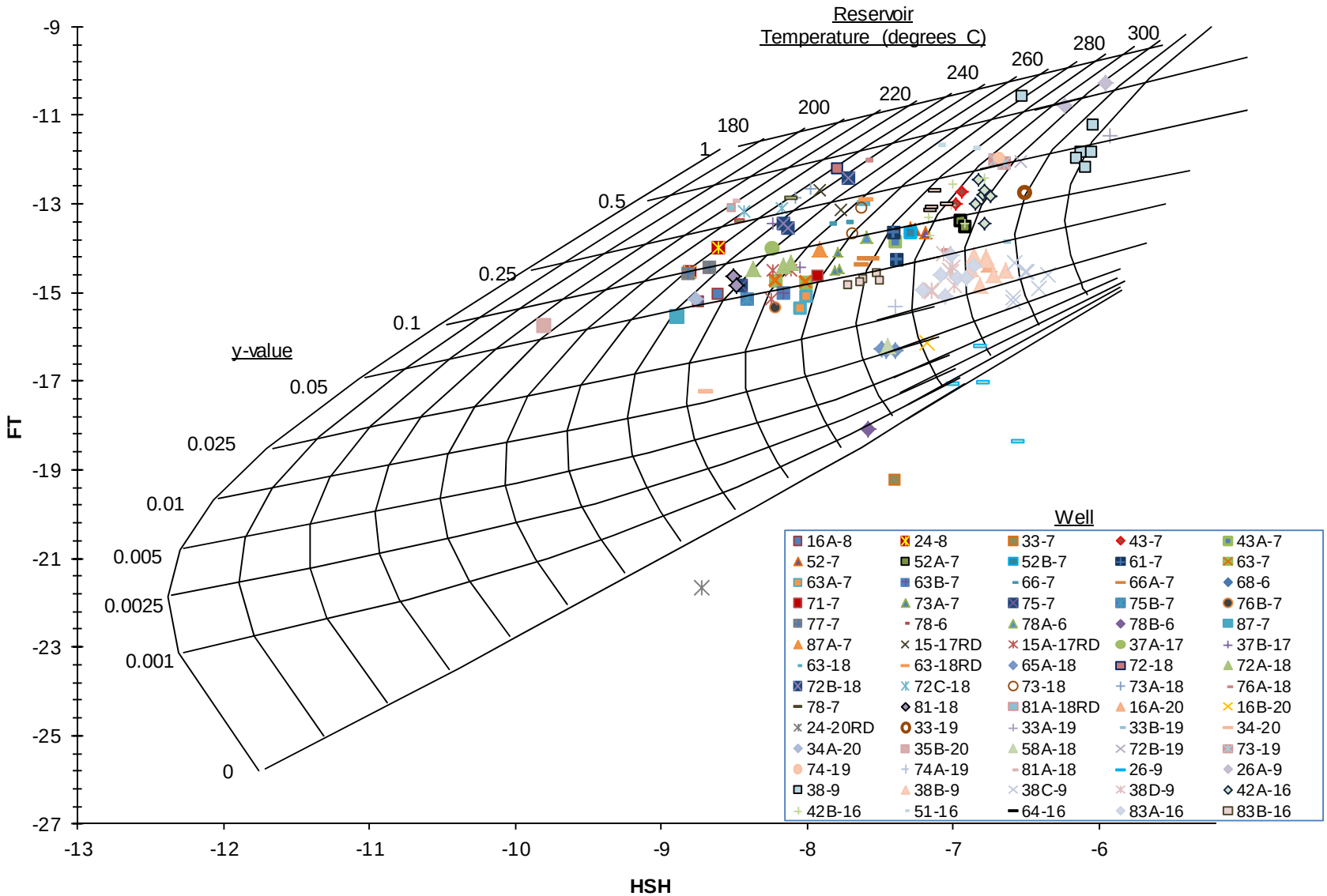

Figure 4-3. Y-grid for 2011 Production Wells (after Truesdell & D'Amore, 1985)

Dynamic temperatures were available from 4 East Flank production wells (26-9, 38B-9, 38C-9 and 83B-16) and 9 west field production wells (16-20, 33-19, 37B-17, 58B-18, 63B-7, 65A-18, 78-7, 81-18, and 87A-7). The East Flank dynamic temperatures are significantly lower (28-47°C; 82-117°F), at an average of 250°C (485°F) than the static (rock) temperatures of 300°C (572°F) to 320°C (608°F). The same is true in the west field with average dynamic temperatures at 210°C (410°F) and static temperatures at 250°C (485°F). Such differences have been observed since the wells were originally drilled and tested.

At least some of this temperature difference reflects reservoir boiling. The pressure and temperature measurements in all wells with dynamic surveys indicate that the wells are essentially two phase within the wellbore. In order to cool fluids to 250°C (485°F), reservoir fluids initially in equilibrium with static temperature of 300°C (572°F) would have to boil 16.5%. At 320°C (608°F), 25% boiling (steam) would be required. Since the rocks would continue to transfer heat to the fluid, actual steam fraction could be higher as boiling continues until all the liquid is gone. In addition, as reservoir pressure declines, boiling increases. When steam passes through hot dry rock, the rocks continue to transfer heat and when there is no more water to boil the steam becomes superheated. Y-grid calculations (see Coso Geochemistry 2007-2010) indicated that the reservoir steam fractions are < 25% in both the East Flank and West Field with the exception of 26A-7, which produces from 50%-100% steam. Therefore steam fractions from Y-grid are consistent with differences between static and dynamic PT survey.

4.4. Mechanism of excess steam

Comparing measured enthalpy to brine Cl (corrected and uncorrected) and G/S in excess steam wells can reflect the mechanism of excess steam. This comparison includes chemical behavior of steam and brine discharges for excess steam wells relative to changes (total enthalpy) as discussed below.

Previous studies (Arnorsson et al., 2007; Henley et al., 1984; Glover et al., 1981) have noted that excess steam can be generated in several ways:

1) Boiling by depressurization and subsequent phase separation of liquid/vapor phases along the flow path to the well (steam added or brine subtracted)
2) Boiling by the addition of heat through conductive transfer from rock to flowing liquid
3) Boiling by the addition of heat through conductive transfer from rock to immobilized water
4) Influx of exotic (not in equilibrium) vapor that is not in equilibrium with reservoir brine. The exotic vapor typically influxes from the edges of the field (Truesdell & D'Amore, 1981).

These processes produce different geochemical patterns:

1) Both G/S in produced vapor and uncorrected Cl remain constant as enthalpy increases, whereas y-total discharge (Y_{TD}) increases since concentrations corrected to reservoir conditions will increase, while the excess steam correction factor will decrease.
2) Conductive heat transfer will increase uncorrected Cl and decrease G/S as degassed brine is boiled. Corrected Cl based on Y_{TD} remains constant, and Cl based on the excess steam correction factor decreases.
3) Assuming the immobilized water re-equilibrated with rock, conductive heat transfer will increase uncorrected Cl. The effect on G/S may be none if equilibrate fluids are similar and the amount of boiling is similar. Corrected Cl based on Y_{TD} remains constant and Cl based on excess steam correction factor decreases.
4) The influx of exotic vapor will not affect uncorrected Cl, but if the vapor is high in gas then G/S will increase or vice versa. Corrected Cl based on Y_{TD} and excess steam correction factor will decrease or remain constant.

The presence of these trends is evaluated in a number of wells (Figure 4-4 and Figure 4-5; Figure A 109 through Figure A 134). Figure 4-4 shows a plot of the parameters discussed above for Well 37-17. Note that with higher measured enthalpy (more excess steam), chloride measured in the brine discharge (uncorrected chloride) remains constant while the corrected chloride decreases and G/S increases. As discussed, this suggests that the increase in enthalpy for 37-17 is related to an influx of exotic vapor higher in gas than steam boiled from in-situ brine.

Figure 4-5 shows a plot of the parameters discussed above for Well 16B-20. Note that as measured enthalpy increases both G/S in produced vapor and uncorrected Cl remain constant, whereas concentrations corrected to reservoir conditions using y-total discharge (Y_{TD}), and the excess steam correction factor decrease. As discussed, this suggests that the increase in enthalpy for 16B-20 is related to boiling by depressurization and subsequent phase separation of liquid/vapor phases along the flow path to the well (steam added or brine subtracted).

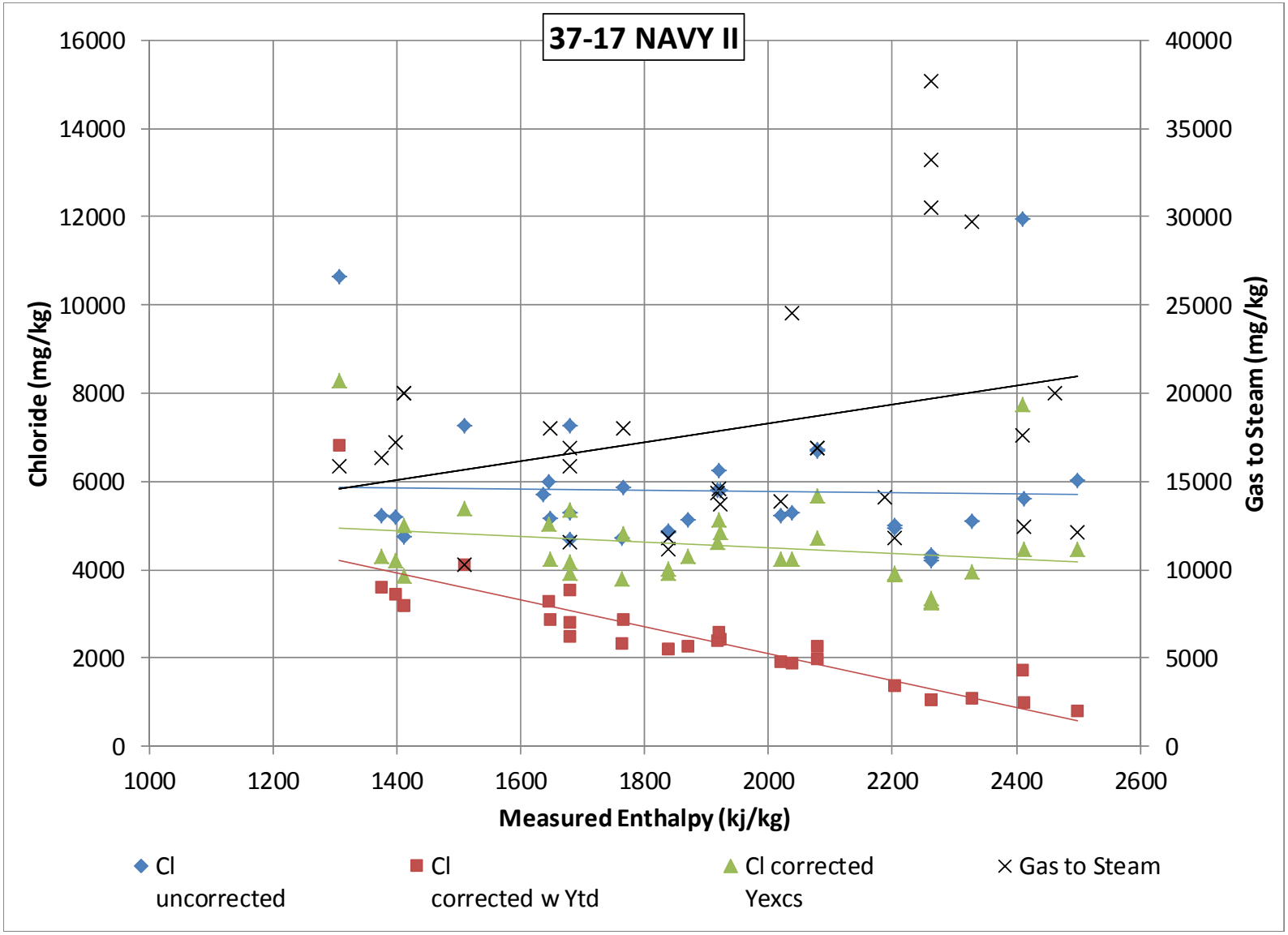

Figure 4-4. Well 37-17 measured enthalpy (kJ/kg) vs Cl in mg/kg in brine and corrected to total flow, and gas/steam (G/S in ppm) in steam

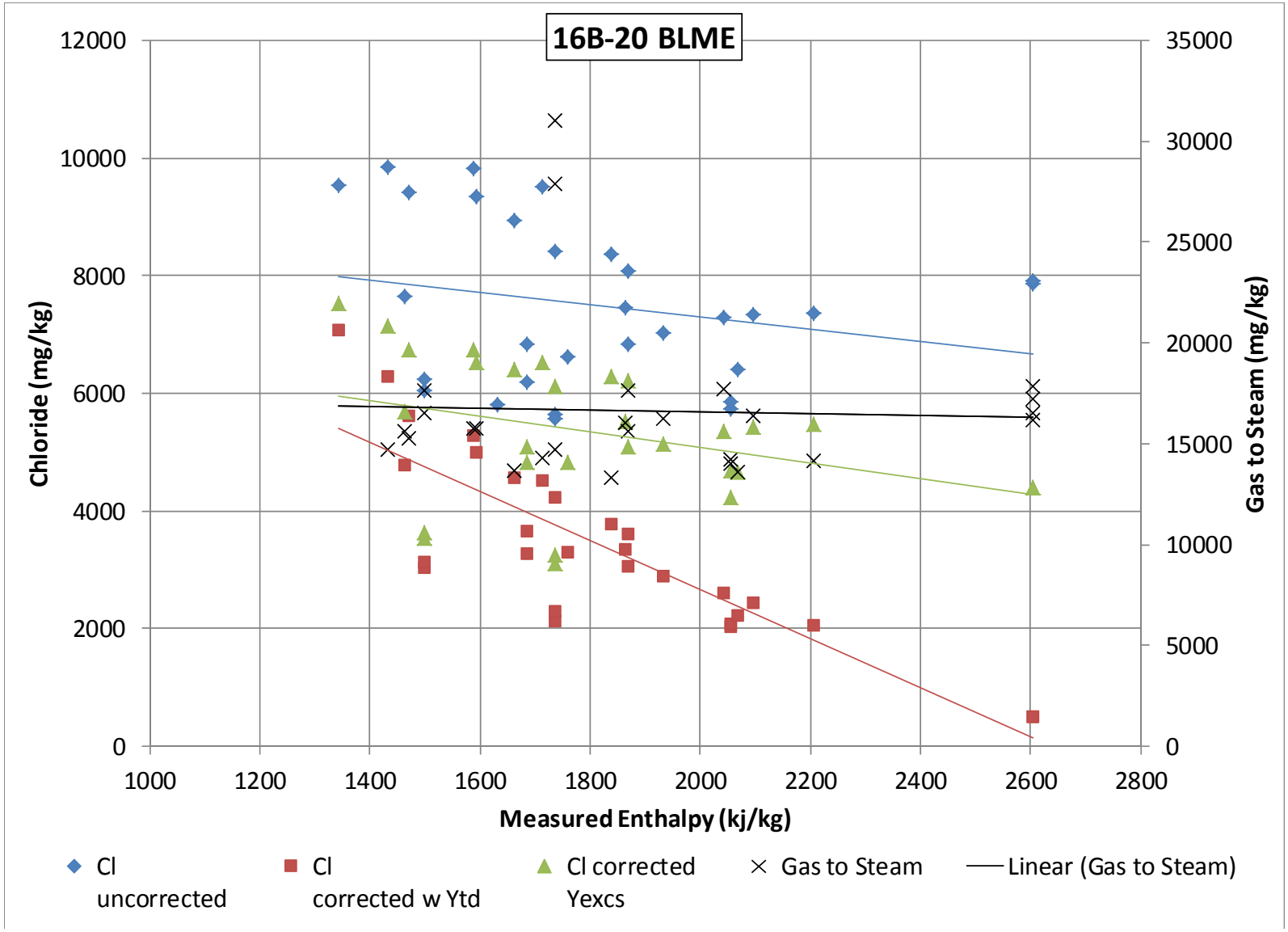

Figure 4-5. Well 16B-20 measured enthalpy (kJ/kg) vs Cl in mg/kg in brine and corrected to total flow, and gas/steam (G/S in ppm) in steam

Because these trends superimpose brine chemistry, steam chemistry, and enthalpy changes, this evaluation of the source of steam is limited to excess steam. In some wells, trends are not clear or vary. But where they are clear, it's possible to distinguish zones where excess steam is (1) related to segregation of phases, (2) produced by vaporization of the flowing fluid, and/or (3) related to an influx of exotic steam. In areas of The Geysers, changes in G/S and steam chemistry have suggested the influx of exotic steam from the edges of the field towards the central low pressure areas (Truesdell & D'Amore, 1981) where pressure declines result from production.

Some patterns have been observed in specific areas of Coso (rather than individual wells) producing excess steam. The source of the excess steam surrounding the central steam zone appears to be phase segregation and addition of vapor in equilibrium with reservoir brine to the well production; vapor is preferentially produced, possibly due to higher relative permeability. In these areas, as enthalpy changes, Cl and G/S remain constant. On the north edge of the steam zone, Cl actually declines while G/S increases with increasing enthalpy suggesting steam condensation or influx of cooler fluids. In southwest edges of the steam zone (BLM East), excess steam appears to be related to the addition of vapor through reservoir boiling, and possibly influx of exotic, higher gas vapor from the edge of the field. In BLM West, lower enthalpy wells appear to have produced excess steam by additional boiling (heat added) possibly of injectate. However, in the far East Flank and in the southwest BLM where enthalpies are highest, the source of excess steam appears to be addition of heat to two-phase flow combined with possible influx of exotic steam.

When boiling continues until liquid is gone, the addition of heat should produce super-heated steam. In these areas where heat is added, wells producing super-heated steam after a period of 100% steam may provide good targets for injection as the chemistry has suggested that the feed zones are hot and dry enough to transfer heat to through steam.

4.5. Reservoir vapor saturation in the reservoir from geochemical modeling

Reservoir saturation was calculated for all production wells where corresponding brine, enthalpy, and gas data sets were available. The saturations were calculated based on the brine, gas, temperature, and enthalpy measurements taken during sampling. These values were input into the WATCH program developed by the Iceland Geochemistry Group in 1982 (Arnórsson et al, 1982). Below are tables of the results for reservoir steam saturation based on the WATCH output for 2010 and 2011.

Table 4-1. WATCH calculated reservoir steam saturation 2010-2011

Well	2010	2011
16A-20	0.43	0.42
16B-20	0.24	0.14
26-9	0.04	0.08
26A-9	0.90	0.82
33-7	0.06	0.00
33-19	no data	0.45
38-9	no data	0.56
38B-9	0.51	0.26
38C-9	0.24	0.16
38D-9	0.42	0.28

Well	2010	2011
42A-16	0.76	0.49
42B-16	0.32	0.10
51-16	no data	0.65
64-16	0.81	0.57
65A-18	0.28	0.15
68-6	0.09	0.00
78B-6	0.00	0.00
83A-16	0.28	0.16
83B-16	0.45	0.20

While reservoir vapor saturation calculated by WATCH has remained fairly consistent in several wells, it appears that overall reservoir vapor saturation is declining across the field, specifically in the East Flank. The Y-grid shows that, in general, most wells across the field have reservoir steam saturations below 25% while the average of the WATCH calculated steam saturations is just over 30%.

These values are consistent with the simple model for producing observed G/S, which suggested 15-40% vapor saturation in the Navy I area and the differences between dynamic and static surveys that suggest 5-20%. Future work to “map” areas of variation in reservoir vapor saturation would include calculating vapor saturation for all wells using multiple methods and contouring the results.

5. Conclusions and next steps

This report presents the geochemical data collected from production and injection wells of the Coso Geothermal System during the calendar year 2011. The data were collected by the Coso Operating Company (COC), and provided to GEOLOGICA by the Navy. GEOLOGICA has evaluated the geochemical monitoring data and assessed variations in geochemical parameters over space and time. This report focuses on using the geochemical data to better understand reservoir conditions such as injection response, temperature distribution, and boiling in the reservoir. Ongoing objectives include using geochemical data to help track the effect of injection on the reservoir conditions in addition to the distribution, breakthrough and returns of the injectate.

This evaluation provided the following conclusions:

- Cl concentrations have remained consistent in reservoir fluid from 2010 to 2011. Some small increases and decreases have occurred that can be attributed to local injectate source and volume. No substantial changes have been observed in BLME, BLMW, East Flank or Navy I. Cl has slightly decreased over time in Navy II since 2010. Since production began, Cl concentrations have been relatively constant in various areas of the reservoir.
- With the exception of extreme spikes related to wells drying out, shifts in Cl concentration trends in production fluid appear to correlate with changes in average Cl concentration levels in injection fluid in the power plant areas.
- Currently, Cl concentrations in the Coso reservoir liquid are ≥ Cl concentrations in injection fluids suggesting that while long term injection recharge produces Cl increases, Cl increases alone can't be attributed to injection breakthrough. These increases could be related to concentration by boiling.
- Historically, Cl/B ratio has been higher in the southern part of the Coso reservoir relative to the central and eastern parts. The Cl/B in the injectate followed the same pattern with the highest Cl/B fluids (waste brine) injected in the south and the highest Cl/B in produced fluids near the injection wells with high brine injection volumes, suggesting that Cl/B reflects injection. In 2011, this pattern changed for injectate but not produced brine; injectate with the highest Cl/B ratios (Hay Ranch water) was injected into the center of the Navy I area and in the East Flank, but the pattern of Cl/B in produced fluids remained unchanged. However, this chemical pattern may provide a tracer of injectate in produced brine.
- The gas/steam (G/S) ratio in produced steam has changed little since 2010. The most significant G/S increases occurred in Navy II. In Navy I, BLME, and BLMW, G/S has remained stable with a small number of wells increasing and a small number decreasing. Decreases may be related to injection derived steam. Across the field, G/S generally continued to increase in the center of the field and decrease on the edges. NCG in reservoir fluid followed a similar pattern.
- H_2S/CO_2 ratios vary significantly across the field, but have not varied over time in individual wells despite changes in boiling and enthalpy. Higher relative concentrations of trace gases on the edges of the field may reflect vapor recharge.

- Ratios of H_2S/CO_2, H_2/CO_2, and CH_4/CO_2 remained high on the outside of the field and low in the center, but showed different patterns. While H_2/CO_2 was highest in the east-north, CH_4/CO_2 was highest in the west and south and H_2S/CO_2 follows enthalpy being higher where wells still produce brine.
- Available isotope data, such as Oxygen-18 ($\delta^{18}O$) and Deuterium (δD) data indicate that using isotopes as injection tracers may require understanding the temperature of boiling and will probably require additional data. Data from 2011 suggests that reservoir fluids boil at approximately 190-200°C (374-392°F).
- Cation (NaKCa) and quartz brine geothermometers remained relatively stable. In the past both geothermometers showed similar spatial patterns, but NaKCa was consistently higher than quartz, suggesting that differences between deep temperatures (NaKCa) and near-wellbore temperatures (quartz) may be narrowing.
- Gas geothermometers remained consistent, maintaining the correlation with measured enthalpy. Enthalpy and the number of steam wells were approximately constant: a small number of wells shifted to steam wells while a small number of steam wells shifted to two phase, resulting in no large net change across the field.
- Evaluation of measured static and dynamic temperatures, brine and gas geothermometers, and measured enthalpy indicate that enthalpy and gas geothermometers appear to reflect the rock temperatures whereas dynamic surveys and brine geothermometers reflect near well reservoir liquid temperatures. It appears that rock temperatures remain high enough to boil reservoir liquid and add excess steam to total fluid discharge.
- Vapor saturation in the reservoir is indicated by (1) "y", calculated using noncondensible gas chemistry (GRID method), (2) differences between dynamic and static feed zone temperatures, and (3) simple mixing to produce observed G/S in the Navy I steam zone, indicate that there is approximately an average 25% by weight vapor saturation in the reservoir.
- Vapor saturation based on WATCH geochemical modeling program indicates that vapor saturation in the reservoir is slightly higher at an average of 30% across wells that possessed enough sampling data to run the program (19 wells across all areas of the field with an emphasis on the East Flank).
- In most of the field, comparison of Cl, G/S and enthalpy suggests that excess steam is produced by adding reservoir vapor that is in equilibrium with reservoir brine to fluid flowing to the wells (as excess steam (enthalpy) increases, chloride and G/S do not). In the East Flank and BLM East, the source of excess steam appears to be additional boiling of fluid as it flows through hot rock (as excess steam (enthalpy) increases, chloride increases and G/S goes either way). These areas may be more conducive to generating injection-derived steam.

In the next year, we propose to continue updating the database and performing the temporal, spatial and geochemical evaluations presented herein. In addition, the following steps will help this geochemical evaluation support resource management at Coso:

1) Evaluate trends in 3-D using "Rockware" and cross sections
2) Compare trends in geothermometers and chloride to assess upflow
3) Refine the interpretation of the vapor saturation and sources of excess steam and extend this work to all wells with brine and steam data using new methods developed by Stephan Arnórsson
4) Use WATCH to evaluate variations in reservoir in addition to vapor saturation
5) Contour vapor saturation along with enthalpy for all methods and compare results to reservoir pressure and enthalpy
6) Map sources of excess steam and compare with enthalpy and, if available, reservoir pressure to understand the possibility of the influx of higher gas steam
7) Continue collecting field-wide stable isotope data. Evaluate the results with respect to known reservoir temperatures, vapor content, boiling, using G/S, geothermometers and the isotopes to further assess the usefulness of stable isotopes to track injection.
8) Update static and dynamic temperatures for wells throughout the field to assess reservoir vaporization
9) Correlate changes in gas and enthalpy over time to distinguish the behavior of gas in vapor-phase sections of the reservoir

6. References

Abrigo, F.V., et al. (2002). Determination of recharge and cooling rates using geochemical constraints at the Mak-Ban (Bulalo) geothermal reservoir, Philippines. Geothermics Vol. 33, pp. 11-56.

Adams, M. C. (1994-2005). Geochemical monitoring of the Coso geothermal system, Prepared for the Geothermal Program Office, Naval Air Weapons Station, China Lake, CA.

Arnórsson, S., & Sigurdsson, S. (1982). The chemistry of geothermal waters in Iceland: Calculation of aqueous speciation from 0° to 360°C. Geochimica et Cosmochimica Acta. Vol. 46, pp. 1513.

Arnórsson, S., & Stefansson, A. (2007). Fluid-fluid interactions in geothermal systems. Reviews in Mineralogy and Geochemistry. Vol. 65, pp. 259-312

Arnórsson, S. (2008). Chemical thermodynamics of two-phase geothermal systems. Preprint.

D'Amore, F. & Celati, R. (1983). Methodology for calculating steam quality in geothermal reservoirs; Geothermics, Vol. 12, No. 2/3, pp 129-140

D'Amore, F. & Truesdell, A.H. (1985). Calculation of geothermal reservoir temperatures and steam fractions from gas compositions; Trans. Geothermal Res. Council, Vol. 9, Part 1, pp 305-310.

Ellis, A. J. & W. A. J. Mahon (1964). Natural hydrothermal systems and experimental hot-water/rock interactions. Geochemica et Cosmochimica Acta Vol. 28, pp. 1323-1357.

Fournier, R. O. (1981). Application of water geochemistry to geothermal exploration and reservoir engineering. Geothermal Systems: Principles and Case Histories. L. Rybach, and Muffler, L. J. P. New York, John Wiley & Sons. pp. 109-143.

Fournier, R. O. & A. H. Truesdell (1973). An empirical Na-K-Ca geothermometer for natural waters. Geochimica et Cosmochimica Acta Vol. 37, pp. 1255-1275.

Geologica, Inc. (2008). Geochemical monitoring of the Coso geothermal system, Prepared for the Geothermal Program Office, Naval Air Weapons Station, China Lake, CA.

Giggenbach, W.F. (1980). Geothermal gas equilibria; Geochemica et Cosmochemica Acta, V. 44, pp 2021-2032

Harper, R. T. & O. T. Jordan (1985). Geochemical changes in response to production and reinjection for Palinpinon-I geothermal field, Negros Oriental, Philippines. Proceedings of the Seventh New Zealand Geothermal Workshop, University of Auckland, Auckland, New Zealand.

Henley, R. H. (1984a). Aquifer boiling and excess enthalpy wells. Fluid Mineral Equilibria in Hydrothermal Systems. El Paso TX, The Economic Geology Publishing Company. Vol. 1, pp. 143-175.

Henley, R. W. (1984b). Chemical structure of geothermal systems. Fluid Mineral Equilibria in Hydrothermal Systems. El Paso TX, The Economic Geology Publishing Company.

Iceland Water Chemistry Group (2010). Iceland water chemistry group presents the chemical speciation program WATCH. www.geothermal.is/software/software

McCartney, R.A. & Lanyon, G.W. (1989). Calculation of steam fractions in vapour-dominated geothermal systems using an empirical method, Proc. 14th Stanford Workshop on Geothermal Reservoir Engineering, Stanford University, Stanford, Calif., pp. 155-161.

McCartney, R.A., & Haizlip, J.R. (1989). Gas pressures at The Geysers geothermal field, California: Comparison with liquid-dominated systems and implications for reservoir conditions, Proc. 14th Stanford Workshop on Geothermal Reservoir Engineering, Jan 1989, Stanford University, Stanford, Calif.

Sullera, M. M. & Horne, R. N. (1999). Inferring injection returns from chloride monitoring data. Twenty-Fourth Workshop on Geothermal Reservoir Engineering, Stanford University, Stanford CA, Stanford University, Stanford Ca.

Sullera, M. M. & R. N. Horne (2001). Inferring injection returns from chloride monitoring data. Geothermics Vol. 30 no. 6, pp. 591-616.

Stefansson, V. (1997). Geothermal reinjection experience. Geothermics Vol. 26, pp. 99-139.

Truesdell, A.H. & Lippman, M.J. (1998). Effects of Pressure Drawdown and Recovery on the Cerro Prieto Beta Reservoir in the CP-III Area; Proceedings. Twenty-Third Workshop on Geothermal Reservoir Engineering, Stanford University.